



저작자표시-비영리-변경금지 2.0 대한민국

이용자는 아래의 조건을 따르는 경우에 한하여 자유롭게

- 이 저작물을 복제, 배포, 전송, 전시, 공연 및 방송할 수 있습니다.

다음과 같은 조건을 따라야 합니다:



저작자표시. 귀하는 원저작자를 표시하여야 합니다.



비영리. 귀하는 이 저작물을 영리 목적으로 이용할 수 없습니다.



변경금지. 귀하는 이 저작물을 개작, 변형 또는 가공할 수 없습니다.

- 귀하는, 이 저작물의 재이용이나 배포의 경우, 이 저작물에 적용된 이용허락조건을 명확하게 나타내어야 합니다.
- 저작권자로부터 별도의 허가를 받으면 이러한 조건들은 적용되지 않습니다.

저작권법에 따른 이용자의 권리는 위의 내용에 의하여 영향을 받지 않습니다.

이것은 [이용허락규약\(Legal Code\)](#)을 이해하기 쉽게 요약한 것입니다.

[Disclaimer](#)

Thesis for the Degree of Master of Engineering

Techno-Economic Feasibility Study for Combined  
Heat, Hydrogen and Power Production (CHHP) via  
Hydrothermal Liquefaction of *Saccharina japonica*.

By

Haider Niaz

Department of Chemical Engineering

The Graduate School

Pukyong National University

February 2019

Techno-Economic Feasibility Study for Combined  
Heat, Hydrogen and Power Production (CHHP) via  
Hydrothermal Liquefaction of *Saccharina japonica*.

다시마의 열수 액화에 기반한 삼중 발전의 기술-  
경제성 타당성 조사

Advisor: Prof. Jay Liu

By

Haider Niaz

A thesis submitted in partial fulfillment of the requirement  
for the degree of  
Master of Engineering

in Department of Chemical Engineering, The Graduate School,

Pukyong National University

February 23, 2019

Techno-Economic Feasibility Study for Combined  
Heat, Hydrogen and Power Production (CHHP) via  
Hydrothermal Liquefaction of *Saccharina japonica*.

A thesis

by

Haider Niaz

Approved by:



---

(Chairman) Jun Heok Lim



---

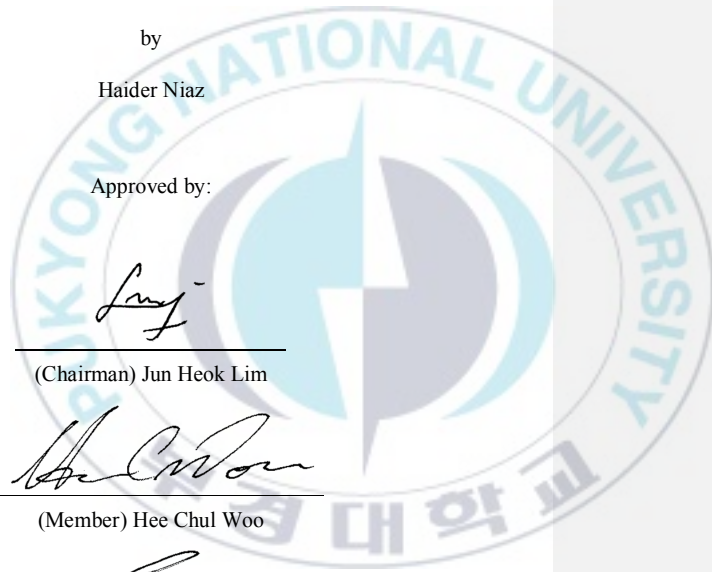
(Member) Hee Chul Woo



---

(Member) Jay Liu

February 23, 2019



**DEDICATION**

*This thesis is dedicated to my parents and my best friend, for their love and support. Every moment of our life together is a beautiful gift. Thanks for being with me.*

## ACKNOWLEDGEMENTS

I would like to sincerely thank my professor, Dr. Jay Liu for the inspiring guidance, encouragement, and exceptional mentoring he has provided throughout my time as his student. I have been extremely lucky to have a supervisor who cared so much about my work and life. I would also like to thank my committee members Professor Jun Hyeok Lim and Professor Hee-Chul Woo.

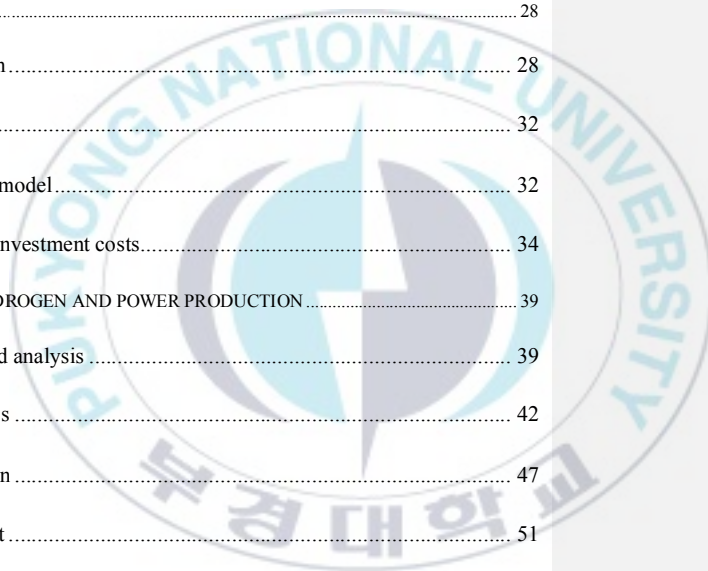
I would also like to thank my parents and my family for their continual support through the years and for encouraging and inspiring me to follow my dreams. I would not be the person I am today if you were not with me during these years. I'd like to express gratitude to my best friend and friends back in Pakistan. I believe all the great moments we have lived together has strengthened our love and commitment for each other.

Finally, I would like to thank all my friends, especially those who live in Busan. Your being here with us made life much more beautiful and happier for us.

## TABLE OF CONTENTS

DEDICATION.....	i
ACKNOWLEDGEMENTS.....	ii
TABLE OF CONTENTS.....	iii
ABSTRACT.....	vi
LIST OF TABLES.....	viii
LIST OF FIGURES.....	xi
1 INTRODUCTION AND BACKGROUND.....	1
1.1. Current energy scenario.....	1
1.2. Importance of biofuels.....	2
1.3. Generations of biomass.....	5
1.4. Algal biomass vs terrestrial biomass.....	6
1.5. Macroalgae.....	7
1.6. Alternate energy production pathways.....	9
1.7. Hydrothermal liquefaction.....	10
1.8. H <sub>2</sub> production technologies.....	11
1.9. Literature survey.....	16

2	EXPERIMENTS.....	19
2.1.	Materials .....	19
2.2.	Characterizations .....	22
2.3.	Liquefaction procedure.....	22
2.4.	Reaction activity tests.....	26
3	SIMULATION.....	28
3.1.	Process simulation .....	28
3.2.	Heat Integration.....	32
3.3.	Technoeconomic model.....	32
3.4.	Total capital and investment costs.....	34
4	COMBINED HEAT, HYDROGEN AND POWER PRODUCTION.....	39
4.1.	Process design and analysis .....	39
4.2.	Design alternatives .....	42
4.3.	Process description .....	47
4.4.	Problem statement .....	51
5	RESULTS AND DISCUSSION.....	52
5.1.	Experiments .....	52
5.2.	Effect of reaction time .....	62
5.3.	Simulation results .....	76
6	CONCLUSIONS .....	98



요약 ..... 100

REFERENCES ..... 103



Techno-Economic Feasibility Study for Combined Heat, Hydrogen and Power Production (CHHP) via Hydrothermal Liquefaction of *Saccharina japonica*.

Haider Niaz

Department of Chemical Engineering, The Graduate School,  
Pukyong National University

**ABSTRACT**

In this thesis, the feasibility study of macroalgae *Saccharina japonica* as a feedstock for hydrogen production was studied. Our study provides a technoeconomic feasibility study for the industrial scale process design for H<sub>2</sub> production via HTL using aspen plus process simulation . Experimental study is performed to analyze various reaction parameters affecting the product phase distribution. The conversion of liquefied oil was found to be maximum of 91.2% at reaction temperature of 300°C, reaction time of 1hr and a macroalgae/water ratio of 1:10. High conversion for the feed was due to high moisture in the feed which supported the dissociation of large molecules. GC-MS analysis for the experimental compounds showed aldehyde and ketones as major functional groups. Best experimental conditions were subjected for process design using process simulator. The goal of simulation study was to evaluate various industrial scale design cases in quest of minimum hydrogen selling price (MHSP). Various design alternatives were taken in consideration to analyze the economics. Design cases were built to minimize the natural

gas utilization and to enhance maximum heat integration. Base case design with external utilities, Case 1: Combined heat, power and hydrogen production (CHHP), Case 2: modified by using fraction of HTL product for combustion. Hot oil system was introduced in the Case 1 and Case 2 as an effective element for reducing the natural gas consumption. Combined heat, hydrogen and power production (CHHP) was simulated using 480,000 kg/yr., of dry *Saccharina japonica*. The process design covered various process section including HTL, steam reforming (SRU), pressure swing adsorption (PSA) and heat and combustion unit. The plant was heat integrated to reduce the total utilities consumption. Net power was produced to make the design self-sustainable. Due to high HHV of 35.5 MJ/kg, case 2 was used to reduce dependency on external utilities via using bio-oil as a combustion fuel. Technoeconomic study was performed to study the feasibility of the process. Economical study revealed that the Case 1 showed the lowest H<sub>2</sub> price of 2.97 \$/kg with an hourly production of 6659 kg/hr of H<sub>2</sub>. Low operating cost and fixed capital investment for the Case 1 in comparison with other design cases make it a suitable design for future assessments.

## LIST OF TABLES

<b>Table 2.1-1.</b> Ultimate and proximate analysis for the macroalgae <i>Saccharina japonica</i> . .....	21
<b>Table 3.1-1.</b> Proximate analysis data input in the process simulator for defining the non-conventional components.....	31
<b>Table 3.3-1.</b> Techno-economic model parameters for the discounted cash flow analysis. .....	33
<b>Table 3.4-1.</b> Cost factors for calculating important costs of the plant's equipment.....	36
<b>Table 3.4-2.</b> Cost factors for estimating the direct and indirect costs.....	37
<b>Table 3.4-3.</b> Material costs for the chemical and raw materials used for H <sub>2</sub> - production .....	38
<b>Table 5.1-1.</b> Characterization of macroalgae with ultimate, proximate and ICP analysis. .....	53
<b>Table 5.1-2.</b> Appearance of liquefaction liquid and solid residue with increasing temperature and at same residence time and feed: water ration.....	56
<b>Table 5.1-3.</b> Effect of reaction temperature on experimental conditions.....	57
<b>Table 5.1-4.</b> Product yields and liquefaction conversion with increasing temperature and fixed reaction time and macroalgae: water ratio of 2 hrs. and 1:10 respectively.....	58

<b>Table 5.1-5.</b> Effect of temperature on carbon conversion in the liquefied oil and solid residue along with mineral content in the liquefied oil and solid residue. ....	59
<b>Table 5.2-1.</b> Product yields liquefaction conversion with increasing reaction time and fixed reaction temperature and macroalgae: water ratio of 300 °C and 1:10 respectively. ....	64
<b>Table 5.2-2.</b> Effect of reaction time on carbon conversion in the liquefied oil and solid residue along with mineral content in the liquefied oil and solid residue. ....	67
<b>Table 5.2-3.</b> Product yields and liquefaction conversion at varying biomass to water ratio at a temperature of 300 C and 1 hr. residence time. ....	69
<b>Table 5.2-4.</b> Organic (bio-oil) compounds distribution for the HTL product liquid mixture at a reaction temperature of 300, 1hr residence time and 1/10 biomass to water ratio. .	73
<b>Table 5.2-5.</b> Aqueous phase compounds distribution for the HTL product liquid mixture at a reaction temperature of 300, 1hr residence time and 1/10 biomass to water ratio. .	74
<b>Table 5.3-1.</b> The stats of current experimental data run from the reduction software...	78
<b>Table 5.3-2.</b> Ready to use reduced mixture along with fractional conversions. ....	80
<b>Table 5.3-3.</b> Summary for the major process input and reaction parameters for the process. ....	85
<b>Table 5.3-4.</b> Installation costs breakdown for the process sections for base case and design alternatives (Case 1 and Case2).....	89
<b>Table 5.3-5.</b> Major material stream for Base Case and design alternatives used in the techno-economic assessment.....	90
<b>Table 5.3-6.</b> Manufacturing cost breakdown for Base Case, Case 1 and Case 2. ....	91

**Table 5.3-7.** Fixed capital investment, and operating cost for design cases. .... 93

**Table 5.3-8.** MHSP calculated for the Base Case, Case 1 and Case 2..... 95



## LIST OF FIGURES

<b>Figure 1.2-1.</b> Biofuel production statistics for the World and South Korea with increasing trend from year 2004 to 2017.....	4
<b>Figure 1.5-1.</b> Different kinds of macroalgae production, highlighting <i>Saccharina japonica</i> with highest production rate.....	8
<b>Figure 1.8-1.</b> Schematic for steam reforming of methane, typical industrial route for H <sub>2</sub> production.....	15
<b>Figure 2.3-1.</b> Separation protocol for the separation of bio-oil and water-soluble organics (WSO) from the HTL product mixture along with separation of the solid product.....	25
<b>Figure 2.4-1.</b> Hydrothermal liquefaction reactor schematic.....	27
<b>Figure 4.1-1.</b> Block diagram for the base case design, which incorporates the combustor unit, which provides heating requirements for all the process sections.....	41
<b>Figure 4.2-1.</b> Case 1, with on-site steam generation and power production. this case incorporates the heat -integration to reduce the consumption of natural gas required for the heating requirements.....	45
<b>Figure 4.2-2.</b> Proposed design for case 2, incorporating liquid product as a combustion fuel for providing heating requirements for the system.....	46
<b>Figure 5.1-1.</b> Effect of reaction temperature of conversion for hydrothermal liquefaction. (Conditions: Feed / H <sub>2</sub> O ratio=1 / 10, Time=2 h).....	60

<b>Figure 5.1-2.</b> Effect of reaction temperature of ash content for hydrothermal liquefaction. (Conditions: Feed / H <sub>2</sub> O ratio=1 / 10, Time=2 h) .....	61
<b>Figure 5.2-1.</b> Effect of reaction time of conversion for hydrothermal liquefaction. (Conditions: biomass / H <sub>2</sub> O ratio=1 / 10, Temperature= 300 °C).....	65
<b>Figure 5.2-2.</b> Effect of reaction time of ash content for hydrothermal liquefaction. (Conditions: biomass / H <sub>2</sub> O ratio=1 / 10, Temperature= 300 °C).....	66
<b>Figure 5.2-3.</b> Effect of feed ratio of conversion for hydrothermal liquefaction. (Conditions: Temperature=300 °C, Time=1 hr).....	70
<b>Figure 5.2-4.</b> Effect of ash conversion for hydrothermal liquefaction. (Conditions: Temperature=300 °C, Time=1 hr).....	71
<b>Figure 5.3-1.</b> GC-MS spectra of the original mixture and the reduced mixture for the organic phase (bio-oil) and the water-soluble phase (Aqueous Phase). .....	79
<b>Figure 5.3-2.</b> Complete process flow diagram for the combined heat, power and hydrogen production via HTL of <i>Saccharina japonica</i> . .....	86
<b>Figure 5.3-3.</b> Single-point sensitivity tornado chart for minimum selling price of hydrogen by varying different variables to see the effect on the hydrogen selling price. .....	97

## CHAPTER I

### 1 INTRODUCTION AND BACKGROUND

#### 1.1. Current energy scenario

According to a survey by United Nations department of the economics and social affairs, its stated that by year 2100, the total population of the world will be approximately 11 billion [1]. With increase in the population , the demand for energy is reaching its thresholds [2]. To support the energy demand, 80 % of today energy demand is supported via fossil fuels. As of now, 55 billion tons of fossil fuels are extracted per year, which is on average is about 10 tons of fossil fuel per person [3]. Such an excessive number of consumption will not only lead us towards the rapid decline of fossil fuel reserves but will also increase the amount of greenhouse gas (GHG) emissions [3]. To support the growing energy demands, alternate energy providers must be fetched [4,5].

Various means of energy are available for energy generation. But the question arises, are they sustainable? When it comes to renewable energy resources such as wind, solar, geothermal energy, they come along with their merits and demerits. Requirement of large area for installation, higher installation costs and restrictions for the geographical locations make them a bit unfavorable. In contrast to this, energy production using algal

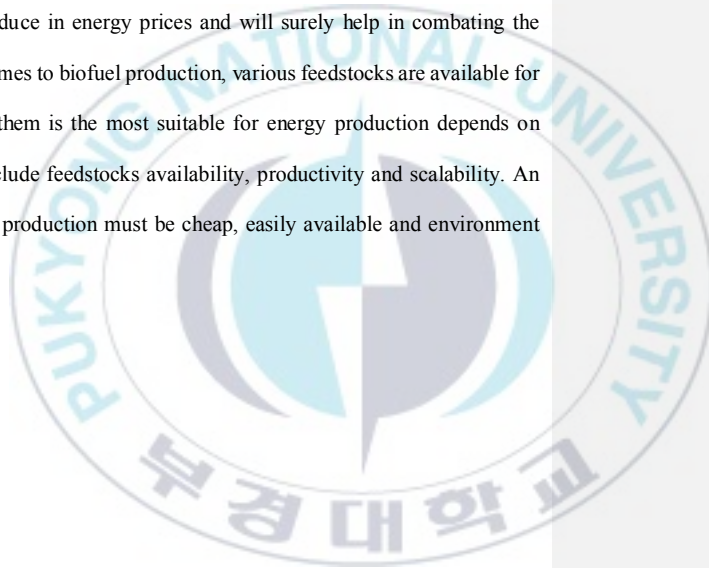
biomass can be a favorable alternative, in context of its availability, higher productivity and no requirements for large land for cultivation [6–8].

Shift of research focus towards biofuel production owes to quest for sustainable energy provider. With the growing demand for energy, alternate energy provider such as biofuels are setting its marks across various parts of the globe. World biofuel production for year 2017 was reported to be 84121 KTOE with an increase of 78% in comparison with 2004 [9]. An increase of 98% was seen in biofuels production for South Korea in year 2017 in comparison to 2004, which clearly depicts the quest for alternate energy resource other than nuclear and fossil fuels [10]. Figure 1.2-1 shows recent trend in biofuel production for the world and South Korea.

## 1.2. Importance of biofuels

Fossil fuels are the primary drivers for the world energy market. By year 2040, approximately 13 billion toe energy will still be provided by the fossil fuels, which is 83% of the total energy demand [9]. So, in comparison to the current energy demand and energy consumption, the reserves for fossil fuels are at an alarming situation. Current world fossil fuel consumption is about 84% of the total world fossil fuel production which is about 5241004 TWh [11]. With such high amount of consumption, the question arises “ Will the global resources last long? ”. With the fact that , fossil fuels are not an infinite resource, and will eventually runout if consumed indefinitely, the answer is “No”. If we look at the reserves to production ratio for various fossil fuel resources such as coal, natural gas and oil , the survey states that we are only left with fossil fuel reserves of 114,

52.8 and 50.7 years respectively [9]. In context to current energy scenario, quest for alternate energy resources such as biofuels impart a great importance towards the goal for a sustainable future. British petroleum's statistical review for the worlds biofuel production shows a raising trend [9]. In year 2017, approximately 600 KTOE biofuel production was observed. Increase in production for biofuels owes to the datum that, biofuels will not only help in reducing increasing energy demand but will also help in securing energy supply, reduce in energy prices and will surely help in combating the climate change. When it comes to biofuel production, various feedstocks are available for the production. Which of them is the most suitable for energy production depends on various factors. Factors include feedstocks availability, productivity and scalability. An ideal feedstock for biofuel production must be cheap, easily available and environment friendly [12].



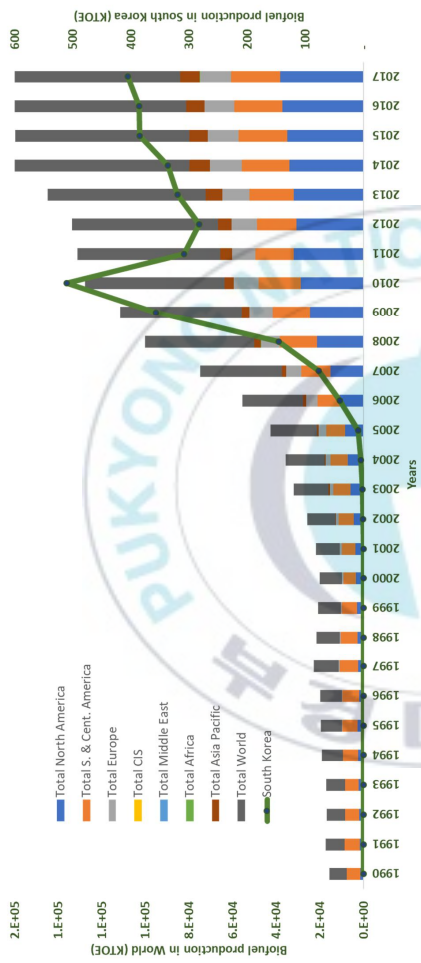


**Figure 1.2-1.** Biofuel production statistics for the World and South Korea with increasing trend from year 2004 to 2017.

### 1.3. Generations of biomass

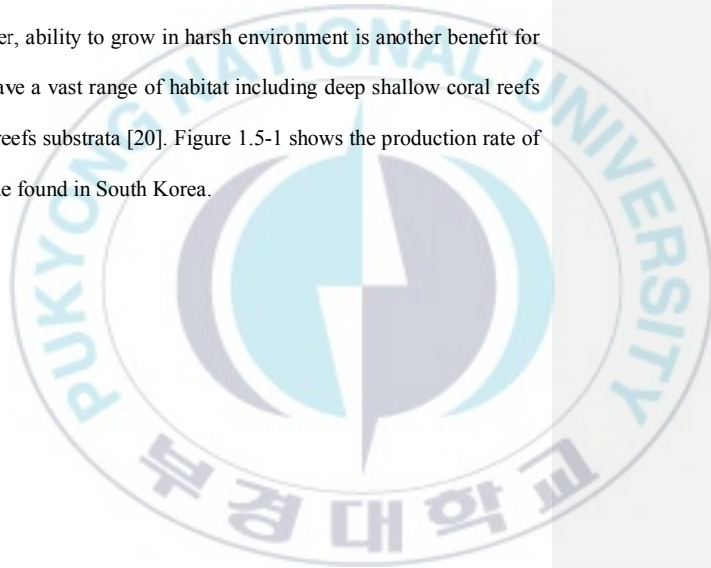
When it comes to biofuel production, which feedstock can be the most promising, depends on the attributes of the individual feedstock. Three different generations of biomass are available for the biofuel production [13–15]. Each of them having their merits and demerits. 1<sup>st</sup> generation biomass comprises of food crops such as sugar, starch, corn etc. The drawback for the 1<sup>st</sup> generation biomass derived biofuels lies behind the fact that they are derived from a food source, its excessive use for energy production will eventually lead us to food crises. This leads us to the 2<sup>nd</sup> generation biomass, which comprises of the non-food biomass including wood, agricultural waste, forest, solid residues etc. Provided with the fact that some of the crops need land for their cultivation (poplar trees), this makes the 2<sup>nd</sup> generation biomass for biofuel production as an unfavorable feed. Finally, 3<sup>rd</sup> generation biomass, such as algal biomass (micro and macroalgae) sounds promising as a feedstock for alternate energy production as it has no competition with the food crops. 3<sup>rd</sup> generation biomass derived fuels are more energy dense in comparison to the other generations of biomass. Their importance is raised due to obvious benefits such as no requirement of land for cultivation, lower cultivation cost, high productivity, can be grown in harsh conditions and have a higher CO<sub>2</sub> reduction rate. The challenge is to find an optimal energy provider to combat the energy demands. Less dependency on resources such as water in terms of production, renewable and no contribution towards climate change makes 3<sup>rd</sup> generation biomass as a promising candidate for energy production [16,17].

#### 1.4. Algal biomass vs terrestrial biomass

Terrestrial biomass, typically the 1<sup>st</sup> and 2<sup>nd</sup> generation biomass can be a source for alternate energy production, but they can't be sustainable in terms of energy production as they are in competition with the food crops. Production of biofuels from terrestrial biomass will certainly raise the risk of deforestation. Increase biofuel production from terrestrial biomass will lead us towards the scarcity for water as the crops need water for their cultivation. Even case for less availability for water, irrigation systems would have to be developed, which will contribute to increase in the production costs. In comparison to algal biomass, all above mentioned attributes are mitigated with the fact that, no requirement of land for cultivation of algal biomass as they grow in the sea. They have higher productivity than terrestrial crops [17–19]. Their ability to grow in harsh environments make them less dependent on the naturally resources such as water. Adverse climate changes due to increase in the fossil fuel usage can be mitigated as algal biomass utilizes CO<sub>2</sub> for cultivation. Higher CO<sub>2</sub> reduction in comparison to other biomass is one of its major contribution towards a sustainable feedstock for biofuel production. Terrestrial biomass have varying harvesting cycles. When it comes to sugar cane, a typical range of 1-2 times/yr. is expected. In comparison to that, algal biomass have higher harvesting cycle typically ranging from 4-6 times/yr. Considering obvious advantages of algal biomass over terrestrial biomass such as ease of cultivation and harvesting, high productivity, and high scalability, they can be a promising feed for alternate energy production.

### 1.5. Macroalgae

Macroalgae (seaweed) are photosynthetic plants with natural abundance due to its production in sea waters. With abilities to grow in sea waters as well as harsh conditions (dirty water) with no requirements of land , macroalgae makes it way towards a suitable candidate as a feedstock for alternate energy. Macroalgae comes in diverse and complex structures. Its complex structure makes it easier to grown in harsh environments. Keeping in mind the scarcity of water, ability to grow in harsh environment is another benefit for macroalgae. Macroalgae have a vast range of habitat including deep shallow coral reefs as wells as inside of other reefs substrata [20]. Figure 1.5-1 shows the production rate of different kind of macroalgae found in South Korea.



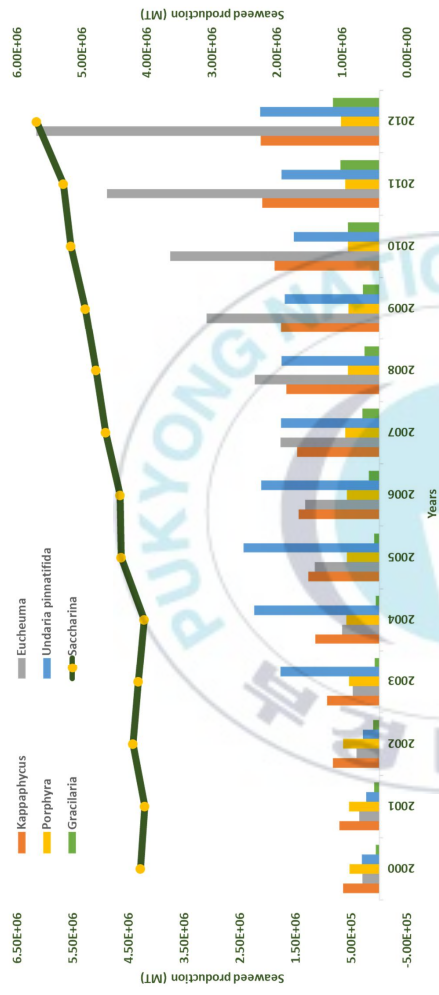


Figure 1.5-1. Different kinds of macroalgae production, highlighting *Saccharina japonica* with highest production rate.

### 1.6. Alternate energy production pathways

Various pathways are available for energy conversion from thermochemical to biochemical pathways. Thermochemical pathways can be classified as gasification, pyrolysis, torrefaction, and liquefaction typically operating between a temperature range from 400-1000 °C and varying pressure conditions. Each technology's approach have their own merits. Biochemical pathway provides higher selectivity's and conversions in comparison to thermochemical pathways, but it isn't enough robust in terms of accepting various feedstocks as thermochemical pathways offer [14]. Provided with the fact that , pre-treatments and fermentation approaches are comparatively costly when it comes to biochemical conversion [14]. On the other hand , requirement of drying in the thermochemical pathway such as pyrolysis makes the process costly [21]. Liquefaction and pyrolysis are the two common thermochemical routes for the conversion of organics in solid biomass into liquid biofuels with some pros on cons. Pyrolysis operates at a relatively higher temperature (450°C-500°C) with a short residence time at atmospheric pressure and requires drying of the feed. Drying of feed makes the process energy intensive which eventually leads to higher production costs. On contrary to this, HTL is carried out at relatively lower temperature (300°C-400°C) with longer reaction time (15min-1hr.) and high pressure (5-20MPa), and doesn't require drying of the feed, which makes it cost-efficient despite of low bio-oil yield. Macroalgae have inherently large moisture content by weight, which is why hydrothermal liquefaction (HTL), which utilizes subcritical water as a reactant presents a viable solution as an energy conversion pathway.

### 1.7. Hydrothermal liquefaction

Hydrothermal liquefaction (HTL) is a polymerization process, in which water at supercritical condition helps in breaking down solid biomass into crude like substance. The presence of water as a solvent in the HTL process eradicates the pre-requisites of drying, which makes it far more flexible in comparison to pyrolysis. HTL product is an energy-dense liquid with equivalent properties to fossil fuels. Inherited moisture of macroalgae serve as a raw material for HTL. Use of water as a solvent has benefits of cost saving when it comes to use of organic solvents, is simple to use and is environment friendly. At standard condition atmospheric conditions, water doesn't react with organics but at sub and super critical temperatures, the properties of water change drastically. Decrease of water's dielectric constant with increase temperature makes the O and H atoms more mobile. Increased temperature results in increased dissociation of  $H_2O$  into  $H^+$  and  $OH^-$  ions, and thus providing more reactivity.

Use of organic solvents has been tested for algal biomass liquefaction to produce more bio-oil with high calorific value, which is predominantly due to removal of oxygen in the form of carbon monoxide, carbon dioxide and water. In terms of high bio-oil yield use of organic solvents can be promising, but for the post processing steps, loss of the organic fraction occurs during the separation of unreacted organic solvent from the HTL product. Along with difficulty in separation, higher raw material cost is another demerit of using organic solvent.

From an economic point of view, hydrothermal liquefaction (HTL) is one of the most promising routes that has drawn attention in recent years for algal biomass as it doesn't require drying of the feed, which itself is an energy-intensive process and thus leads to a higher production cost. Ability to handle wet feedstock, higher bio-oil heating values ranging from 35-39 MJ/Kg and yielding a liquefaction efficiency of 85-90% give HTL an upper hand among thermochemical technologies.

#### 1.8. H<sub>2</sub> production technologies

Up till now, various technologies are available for H<sub>2</sub> production, each of them with their own merits and demerits. In today's world, the technology with better efficiency and lower production cost will be the optimal choice. Various raw materials are available which can be a source of H<sub>2</sub>, but the question arises, will they be economical and sustainable? To evaluate the question, we can compare various technologies. Water, natural gas, biomass (algal and terrestrial biomass) and fossil fuels are some of the common raw materials which can be employed for the H<sub>2</sub> production. Various methods which can be used to produce H<sub>2</sub> includes the following:

- I. Electrolysis (Electric current decomposes the water into hydrogen and oxygen which then leads the electrochemical reactions)
- II. Plasma arc decomposition (H<sub>2</sub> is produced by passing plasma arc through pure methane)
- III. Thermolysis (Steam at ultra-high temperatures of 2200 °C decomposes water into its constituents)
- IV. Gasification (Biomass gasification)

V. Reforming (Liquid organic fuels are breakdown for H<sub>2</sub> production)

VI. Dark Fermentation (Anaerobic fermentation of biomass in absence of light to produce H<sub>2</sub>)

Considering the demerits for few of the above-mentioned technologies, we can say that, a process can't be sustainable if it requires the expenditure of large amount of energy and heavy investment for the safety of its equipment and handling. For the process to be economically viable, the technology must be cheap and readily available with minimum investments. Plasma arc decomposition can generate very high temperatures using electricity, but it comes with a disadvantage of dependency on electricity along with increased electrode erosion. Increased electrode erosion is a resultant of the high pressures and less mobility of the arc. Hence decreasing the electrode lifetime. So then comes the steam reforming of the liquid organic fuels obtained from the thermochemical conversion of the biomass. Typical methods used in this context includes pyrolysis, gasification and hydrothermal liquefaction. Gasification does provide H<sub>2</sub> but when it comes to separation, drying of wet feedstocks, removal of tar to a significant level for pure H<sub>2</sub> is challenging. The difficulty in achieving pure hydrogen lets down gasification from getting recognition at industrial scale. In case of pyrolysis, potential for fouling via produced carbon makes pyrolysis unfavorable but appropriate designs can minimize it. High energy requirements for the pre-treatment of the pyrolysis feed can be costly which makes it less viable. So, it leaves us with the liquid product obtained from the HTL. Brief introduction to steam reforming is provided in section 1.8.1.

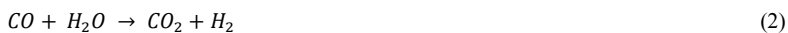
### 1.8.1. Steam reforming

**Figure 1.8-1.** Schematic for steam reforming of methane, typical industrial route for H<sub>2</sub> production. shows graphical representation for a typical steam reforming process flow. A common method for producing H<sub>2</sub> from carbon containing compounds. Methane reforming is one of the most industrially used process for H<sub>2</sub> production. Steam reforming utilized steam to break down the organics into syngas (CO+H<sub>2</sub>). A process in which , organics react with steam at high temperature in presence of a metal catalyst to breakdown into components comprising of CO and H<sub>2</sub> primarily and trace amounts of other gases including CO<sub>2</sub> is referred as steam reforming. During steam reforming, water gas shift reaction takes place, which converts CO into CO<sub>2</sub> hence providing more H<sub>2</sub>. H<sub>2</sub> on later stages is separated from other gases and is compressed and stored. Steam reforming is an endothermic process, which means it needs a constant supply of heat to maintain its operation. As we know, to obtain H<sub>2</sub> a fuel source must be present, which in case of methane steam reforming is methane. In case of HTL, the bio oil coming from the HTL product serve as a raw material and are reformed using steam to produce H<sub>2</sub> and CO. The typical reactions which take place in course of steam reforming are mentioned in eq (1) and eq (2)

Steam – reforming reaction

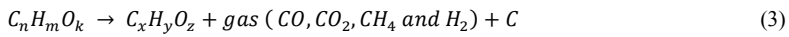


Water gas shift reaction



Other reactions that take place during steam reforming are mentioned as under:

Thermal decomposition reaction



Methane steam reforming



Boudouard reaction



Carbon deposit gasification



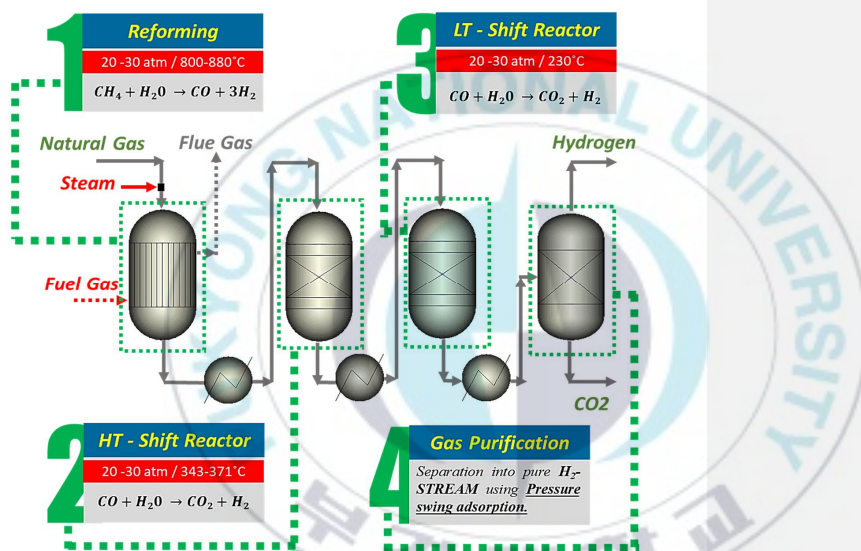


**Figure 1.8-1.** Schematic for steam reforming of methane, typical industrial route for  $H_2$  production.

### 1.9. Literature survey

Various studies are performed to evaluate the performance of HTL based on reaction parameters and various solvent. The effect of HTL conversion has also been studied with reference to with and without catalyst. Zhou et al. studied the HTL of *Enteromorpha prolifera* at a temperature of 300°C using ethanol as a solvent for a reaction time of 15 minutes with feed to solvent ratio of 1:10. He reported liquefaction conversion of 57% and a bio oil yield of 7.95 wt.%. He also investigated the conversion using methanol as a solvent and achieved 1% increase in the conversion with relatively lower bio-oil yield of 44 wt.% [22]. Singh et al. carried out HTL using *Ulva fasciata* with 3 different solvents water, ethanol and methanol at a temperature of 300°C, 7-9 MPa pressure and reaction time of 15 minutes in absence of catalyst. Highest conversion of 76% was achieved using water as a solvent with a lowest conversion of 59% reported for ethanol. Contrary to that bio-oil yield for water as a solvent was 15 wt.% relatively lower in comparison with the ones obtained with organic solvent which was 54 wt.% and 59 wt.% respectively [23]. Chen et al. reported that he observed higher bio oil yield than the amount of lipids present in the feed, which led him to conclude that, other organic species also contribute towards the bio oil yield [24]. Zeb et al. achieved a bio-oil yield of 16 wt.% and 19 wt.% using water as a solvent at sub-critical (300°C) and supercritical (400°C) water conditions, respectively with 1:10 ratio of *Saccharina japonica* to water [25]. HTL using organic solvents was also studied by Zeb et al., reporting a demerit of difficult separation of organic solvents and loss of bio-oil during separation [26,27]. Ross et al. carried HTL with 4 different macroalgal species, *L.hyperborea*, *L.saccharina*, *L.digitata*, *A.esculenta*

with a feed of 8g and 30ml of water at 350°C and 15 min residence time, yielding bio-oil of 9.8-17.8wt.% [28]. Neveux et al. reported bio-oil yields for 6 different types of feedstock using marine water and freshwater as solvent with biomass to solvent ratio of 0.07, residence time of 5 minutes and a temperature of 330 °C [29]. Highest bio-oil yield of 26.8wt.% was achieved with fresh water *Oedogonium* macroalgae and a lowest yield of 9.7wt.% using marine algae named *Chaetomorpha* [29]. Singh et al. performed HTL of three different macroalgae (*Ulva fasciata*, *Sargassum tenerrimum*, *Enteromorpha* sp.) with biomass to water ratio of 0.16 at a temperature of 280°C with a residence time of 15 minutes. Liquefaction conversion of 67%, 77%, and 81%, and bio-oil yield of 7, 9, and 12 wt.% were reported, respectively [30]. Experimental data still lack for the HTL of macroalgae using water as a solvent at autogenous pressures. Recent studies on HTL of macroalgae performed at various operating conditions show that feed to water ratio, reaction time, and pressure greatly affected the liquefaction conversion. Feasibility study for industrial scale design of HTL using microalgae is available but for macroalgae it's still scarce [31–33]. Various studies report HTL of macroalgae yielding high bio-oil yields but have lower liquefaction conversions at higher pressures of 20 MPa [9,30]. More specifically for the course of our interest, studies report HTL of *Saccharina japonica* at high pressures (20 MPa) but only a few literature studies are available on HTL at autogenous pressure conditions with no economic feasibility models [12,13,34]. Therefore, we studied the effect of various reaction parameters at lower liquefaction pressures on raw-biomass conversion and bio-oil yield. Our experimental study thus provides a support for HTL with higher conversion and relatively higher bio-oil yields in

comparison to previous studies while using raw-biomass at autogenous pressure conditions. Experimental studies will lack their importance if they don't have their supporting economic studies available to evaluate these processes on industrial scale. Apparent gaps for the assessment of macroalgae as a feedstock for large scale production of biofuels via HTL are present now. Thus, to bring these technologies into reality, economic studies are required for better estimation of their viability at industrial scale. Therefore, our study tries to bridge the gaps by providing an economic feasibility study for industrial scale process design for HTL of macroalgae based on experimental data from HTL of *Saccharina japonica* at autogenous pressure. Experimental study evaluates the highest conversion obtained for HTL based on reaction parameters. Industrial scale process design for CHHP is evaluated for downstream hydrogen production via steam reforming of the bio-oil. Process design involves heat integration with the major process sections i.e. HTL, SRU for steam generation and feed pre-heating for the HTL and steam reforming unit (SRU). Keeping in mind the power requirements, on-site steam is generated from hot streams. Surplus high-pressure steam is used for power generation using steam turbine. Research innovation behind the process design for H<sub>2</sub> production via HTL of macroalgae is to make it self-sustainable by using minimum utilities and by conserving energy. A separate case scenario is evaluated in which part of bio-oil stream is utilized for replacing natural gas for combustion purposes. Cost is evaluated for various design cases to understand process economics and profits in a better way. Later, MHSP of H<sub>2</sub> is compared for various design case scenarios for choosing the optimal design.

## CHAPTER II

### 2 EXPERIMENTS

#### 2.1. Materials

The raw macroalga, *Saccharina japonica*, as a feedstock was collected from a testing farm near Wando Island, Republic of Korea. The raw macroalgae was dried in sunlight reaching to a moisture content of 10-15% and was later dried at 105°C for 12 hrs. in a drying oven. Later, the feed was ground to obtain a particle size of 1-3mm using a knife mill. The major composition for the organic content were carbohydrates (67%), proteins (14.8%) and lipid contents (around 2.4%). Because composition of macroalgae changes with season, one batch of feedstock was used for all the experiments to ensure consistency. Ultimate and proximate analyses results of the raw macroalgae are presented in Table 2.1-1. HPLC-grade acetone and dichloromethane (DCM) were purchased from Sigma Aldrich Korea.

The experiments were carried out in a stainless-steel reactor ID43 x 115L with a design capacity of 120cc and an operating capacity of 100cc. The operating temperature and pressure were 450 °C and 150 kg/cm<sup>2</sup> respectively with a design capacity of 500 °C temperature and 180 kg/cm<sup>2</sup> of pressure. Digital type pressure transmitter and a bourdon gauge with a range of 0~200 kg/cm<sup>2</sup> was used to note the pressure. Relief type pressure

safety valve was used with the relief point of 180 kg/cm<sup>2</sup>. K-type thermocouple was used to measure the temperature. Furnace heater was used with a capacity of 2.5 kw with a ceramic board and 304SS case insulation. An amount of 6g of biomass was weighed and loaded in the reactor, followed by an addition of 60ml of water to reach a biomass/water ration of 1:10. The reactor was then sealed and airtight. The experiment was repeated at varying time (1-4 hrs.), temperature (280-300 °C) and biomass/water ratio (1:5, 1:7, 1:10) with 10.0 to 85.9 bar of autogenous pressure at respective temperatures. Liquefied oil was prepared by the instrument shown in Figure 2.4-1.

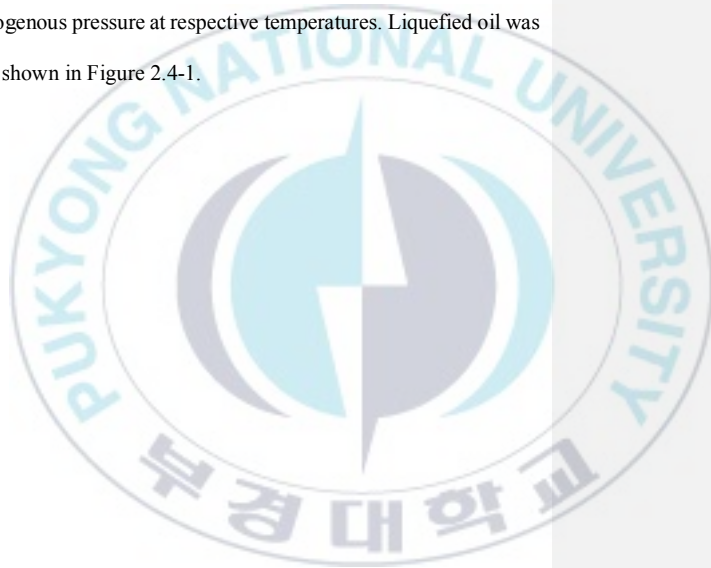


**Table 2.1-1.** Ultimate and proximate analysis for the macroalgae *Saccharina japonica*.

Ultimate analysis					
C	H	N	S	O	HHV (MJ Kg <sup>-1</sup> )
38.17	4.76	2.17	-	54.9	24.41
Proximate analysis					
M	VM	FC	Ash <sup>1</sup>	Ash <sup>2</sup>	
5.78±1.5	68.41±1.6	4.27±1.2	21.54±1.0	23.78±1.0	

<sup>1</sup>Analyzed by TGA (900°C, 10°C/min)

<sup>2</sup>Ash analysis by ASTM E-1755 method.

## 2.2. Characterizations

The proximate analysis of solid residue after HTL was conducted according to the ASTM standard methods of E 1755, and 1756. The water contents of bio-oil and WSO were analyzed through Karl-Fischer titration according to the ASTM standard E-203 method. The elemental compositions (C, H and O) of the liquid product (bio-oil + WSO) and the solid residue were determined by using an elemental analyzer (FLASH 2000, Thermo Scientific: FLASH 1112 series) in accordance to the ASTM standard methods of D 5291, and D 5622.

## 2.3. Liquefaction procedure

Liquefaction experiment was performed using a SS-316 reactor system with a 316-L magnetic drive. Reactor's working volume was 100cc with a safe operating pressure and temperature limit of 150 kg/cm<sup>2</sup> and 500°C, respectively. Reaction temperature was achieved using a furnace heater with 2.5 kW heating capacity insulated with ceramic board of 304-SS material of construction (MOC). Digital pressure transmitter and a bourdon gauge with a range of 0-200 kg/cm<sup>2</sup> were used for pressure readings. K-type thermocouple with 316-L MOC was employed for temperature measurement. Digital PID controllers were used to control both temperature and pressure according to the reaction conditions. RPM was controlled using an inverter driver.

Steps for separation protocol are shown in Figure 2.3-1. Separation protocol for the separation of bio-oil and water-soluble organics (WSO) from the HTL product mixture along with separation of the solid product. Steps for the conversion of the raw biomass

into end products are shown in Figure 3. Dried biomass was used from previously dried batch of *Saccharina japonica* kept for experimental purposes. After adding 5.4 g of biomass and 54 ml of water to keep biomass to solvent ratio of 1:10, the total weight of reactor including the feed was measured. The reactor was heated to the desired temperature of 300°C with a heating rate of 3.5°C/min. After the desired temperature, the reactor was kept at constant temperature of 300°C for 1 hr. The reactor was cooled at room temperature gradually with time. After cooling, the reactor was weighed prior to extraction of the product after venting the gas. The difference in the weight of reactor was considered as the weight of a gas product.

Liquid product from the reactor was mixed with dichloromethane (DCM) as a rinsing solvent for further processing. The DCM and product mixture was later filtered using a Buchner funnel connected with an aspirator. The solid residue collected on the filter paper was dried in an oven at 105°C. The filtrate collected formed two phases and later was separated using separating funnel. Top layer was the organic phase (bio-oil) and the bottom layer was the aqueous phase containing water-soluble organics (WSO). Both layers were separately collected for further processing. Aqueous phase was kept in a drying oven at 60°C for 12 hrs. Difference in the initial and final weight of the aqueous product yielded the WSO. Some of the product was still on the walls of the reactor and the stirrer. The reactor was cleaned using acetone as a solvent. The liquid collected from the reactor cleaning was filtrated using a Buchner funnel, similarly, the solid residue collected was dried in drying oven at 105°C for 12 hrs. Later both solid residues were collected and weighed, providing the total solid product of the reaction. The filtrate

collected after filtration of acetone mixture was mixed with the organic phase collected from the separating funnel. Later it was subjected to rotary evaporation at a temperature of 30°C to evaporate all the solvent and was kept for 1 hr. The difference in the weight of round bottom flask before and after was recorded for calculations of remaining bio-oil to avoid errors due to adhesion with the walls.

The weight conversion of macroalgae, solid residue and gas were calculated as under using equation (7-9) respectively:

$$\text{Liquefaction conversion (\%)} = \frac{\text{Weight of feed} - \text{weight of solid residue}}{\text{Weight of feed}} \times 100 \quad (7)$$

$$\text{Solid residue (wt. \%)} = \frac{\text{Weight of solid residue}}{\text{Weight of feed}} \times 100 \quad (8)$$

$$\text{Yield of gas (wt. \%)} = 100 - \text{sum of (solid residue + liquefied oil) wt\%} \quad (9)$$

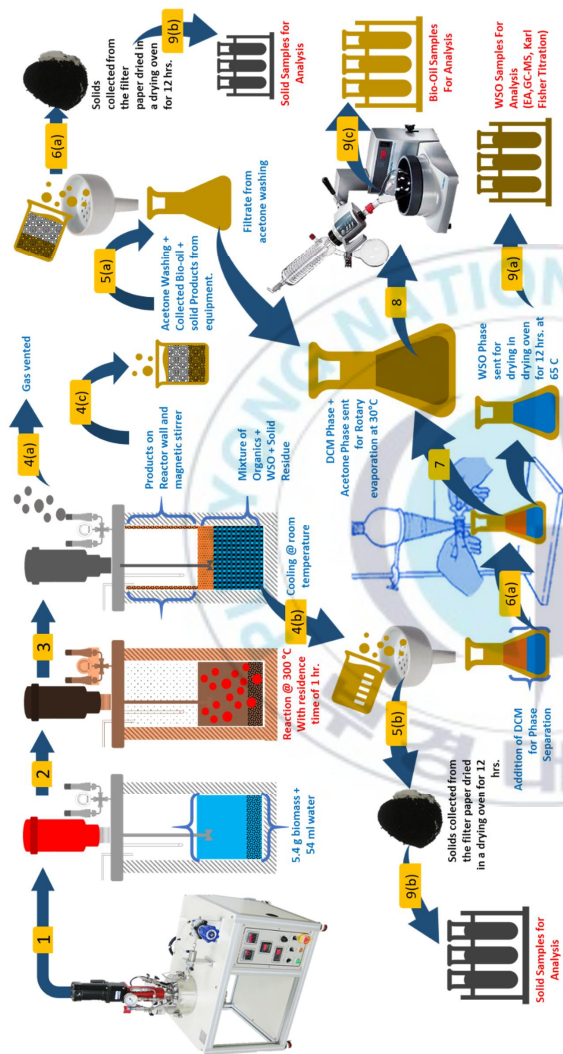


**Figure 2.3-1.** Separation protocol for the separation of bio-oil and water-soluble organics (WSO) from the HTL product mixture along with separation of the solid product.

#### 2.4. Reaction activity tests

To understand the reaction mechanism in a better way, effect of various parameters on the liquefaction conversion and bio-oil wt.% was studied. HTL experiments was performed at various conditions of temperature, feed: water ration and residence time. Other factors such as effect of solvent on the conversion and bio-oil wt.% was not studied in this study. To justify the claim for the effects of reaction parameters, HTL was studied for a temperature range of 180-300 °C , with an interval of 40 °C for every set of experiment. The initial starting points for the residence time and feed: water ratio were taken as 2hr. and 1:10. Effect of residence time was studied for a period of 1,2, and 4hrs. For each set of conditions, the conversion as well as the weight distribution for the phases varied. To evaluate the effect of biomass: water ration, ratio of 1:10, 1:7, and 1:5 were studied. With the fact that high amount of moisture yields a higher conversion. All these conditions were studied during reaction activity tests [31].

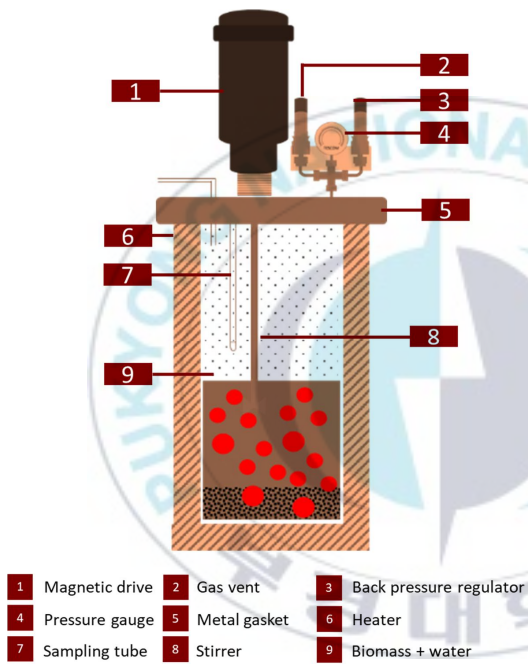


**Figure 2.4-1.** Hydrothermal liquefaction reactor schematic.

## CHAPTER III

### 3 SIMULATION

#### 3.1. Process simulation

A process simulation software helps you create a process model. A process model is defined as a complete layout of an engineering system comprising of :

- I. Flow sheet
- II. Chemical component
- III. Operating conditions

The process simulator helps in designing, developing, analyzing and optimizing of the chemical plant and processes by providing approximate estimation for real time data. Aspen plus calculates rigorous material and energy balance keeping in consideration the thermodynamics for every unit operation. Various studies covered HTL of biomass and other thermochemical routes using aspen plus simulation software [6,21]. All processes in consideration with respect to this study are simulated using Aspen plus.

To work with aspen plus, user must input the compounds available or which will be used during the simulation. These compounds include solids, gas and liquid. Aspen plus provides a data base of most of the chemical compounds. Compounds can be searched

and used by entering their names or by entering their associated CAS no. There is another category for the solid compounds which are not available in the aspen compound data base termed as non-conventional components. For the non-conventional components, specially defined properties are used in order to incorporate them in the process simulator. These compounds are defined based on the properties such as proximate, ultimate and sulfanal analysis. In comparison to general chemical components in the aspen data base, non-conventional components are defined by different set of property methods depending upon their chemical properties. In our case, biomass, *Saccharina japonica* and ash are considered as non-conventional components. These compounds are defined using their elemental and proximate analysis. Furthermore, special set of property methods such as DCOALGIST and HCOALGIST are used to define their density and enthalpies correlation. Property methods used for the other components include NRTL and SRK-KD. These property methods are efficient in terms of estimating and calculating properties for the organic mixtures at high temperature and pressures. The NRTL activity coefficient ( $\gamma_i$ ) model can represent highly non-ideal liquid mixtures at low pressures too. In our study we used these methods at alternate locations for estimating accurate data.

The non-conventional components used in this study are *Saccharina japonica* and ash. The properties for these solid compounds are defined using the analysis mentioned in the previous section Table 3.1-1. Table 2.1-1 and Table 3.1-1 shows the non-conventional components modelled in our study using proximate and ultimate analysis respectively. Macroalgae was assumed as a raw macroalgae, which on collection for the islands contains a moisture of 85-90%. To replicate the sulfur guards, we used simple separators

for the separation of sulfur and other impurities from the desired stream. The costs involved with the industrial scale design for those separators is included in the techno-economic assessment. The HTL reactor is modelled as R-STOIC reactor. To simulate the HTL reaction you must either provide reaction kinetics or the respective conversions. In our case we modelled using the conversions of the experimental compounds provided by the GC-MS analysis. It can model the reaction occurring both sequentially and simultaneously. It also can help in calculating the heat of reaction. For SRU, we used R-Gibbs reactor. This reactor type doesn't require reaction stoichiometry. It models the reactor using phase and chemical equilibrium. For the steam reformer, we set the option to restricted chemical equilibrium with specified temperature approach or chemical reaction. We provided the chemical reactions that occur during steam reforming reaction. For the high and low temperature water gas shift reaction we modelled using R-Equil. This specific reactor type uses the reaction that takes place during the process. PSA was modelled as a simple separator, based on the industrial scale design, 15 % of the H<sub>2</sub> was recycled back to the process for purification and for bringing into account the fact the separation efficiency is not 100%.

**Table 3.1-1.** Proximate analysis data input in the process simulator for defining the non-conventional components.

Parameters	Biomass	Solid residue
Moisture	5.78	8.72
Volatile matter	68.41	50.59
Fixed carbon	4.27	8.52
Ash <sup>1</sup>	21.54	32.17

<sup>1)</sup> Analysis by TGA (900°C, 10°C/min)

### 3.2. Heat Integration

For every process to be economical and viable, deep concerns are raised based on the energy consumption and respective profits generated from the process. In order to cut short, the excess heating and cooling requirements of the process, heat integration plays its role by minimizing the heating and cooling demands. Heat integration integrates the process in a way that hot streams provide enough heat for the stream that require cooling and the cold streams that need to be raised to a certain level of temperature are pre-heated by the hot stream from the process. For the remaining energy, which is required for the reaction conditions is met by additional heat source which can be either a combustor, fired or electric heater or a furnace.

### 3.3. Technoeconomic model

Modified accelerated cost recovery system (MACRS), which considers zero salvage value, was used to determine the federal taxes to be paid. It was assumed that 4 months of startup period, an average of 50% production could be achieved while incurring 75% of variable expenses and 100% of fixed expenses. Table 3.3-1 shows the technoeconomic parameters selected for the total plant cost evaluation.

**Table 3.3-1.** Techno-economic model parameters for the discounted cash flow analysis.

Parameter	Value
Cost year of analysis	2018
Internal Rate of Return	10%
Plant financing/debt equity	1
Plant Life	30 years
Income tax rate	21%
Startup time	0.25 years
Working capital	5 % of FCI
Construction period	3 years
Plant salvage value	No value
Costs during startup	Variable costs = 75 % Fixed costs = 100 %
Indirect Capital Cost	55 % of the TIC

### 3.4. Total capital and investment costs

Material and energy cost calculations were estimated using Aspen plus simulation. Based on these values' approximation for the number of equipment's required to support the economic model were estimated. The cost for the equipment were calculated based on the data from the literature [6]. Base equipment cost for the quoted values from the literature were adjusted to our study's values using the following equation :

$$\text{Scaled equip. cost} = \text{Equip. Cost in quoted Year} * \left( \frac{\text{Scale up capacity}}{\text{Original capacity}} \right)^n \quad (10)$$

Where “n” is the scaling exponent available in literature for various equipment's. This study used the exponent values from the PNNL report and Turton et al [6,32]. Detailed descriptions for the scaling exponents and installation factors were available in the PNNL report. Some of the costs were provided as a complete unit. For such cases, we estimated the cost from aspen cost estimator and evaluated the individual cost for the specific equipment from other mentioned literature [33].

Table 3.4-1 gives the cost factors for calculating the cost for the important equipment's of the plant. The costs mentioned were for different years, to convert those costs for the year 2018 costs, following conversion equation was used :

$$\text{Cost in Current Year (X)} = \text{Equip. Cost in quoted Year} * \frac{\text{Current year CI}}{\text{Quote year CI}} \quad (11)$$

Direct and indirect costs accounted for the fixed capital investment of the plant. Table 3.4-2 gives the cost factors for the direct and indirect costs. Operating costs included the fixed and variable operating costs. Fixed operating costs covered entities like salaries of employees ( Managers, technicians, shift operators etc. ). Variable operating costs included the costs for the raw material, chemicals, utilities etc. Prices for the chemicals and raw material were taken from various literature studies [6,32,34–38]. Unit costs for the variable operating parameters is shown in Table 3.4-3.

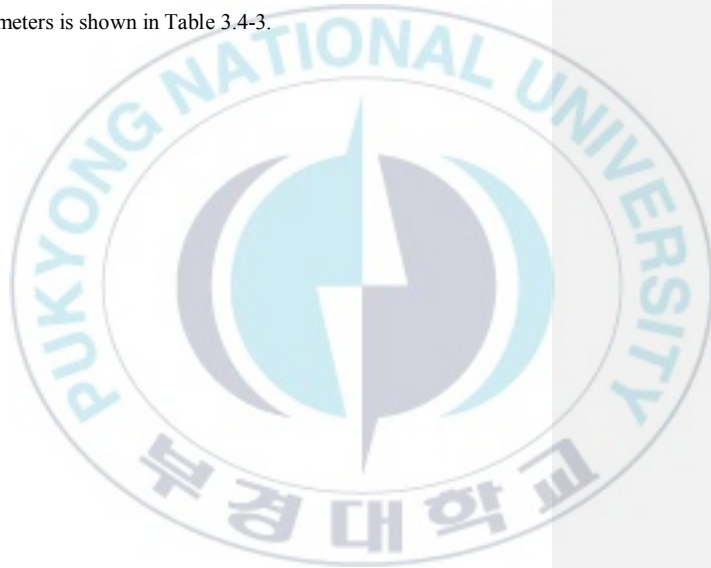


**Table 3.4-1.** Cost factors for calculating important costs of the plant's equipment.

Item	Base Year	Scaling Exponent	Install Factor	Ref.
Feed Crusher	2012	0.85	3.02	[39]
Feed Pump	2011	0.8	2.3	[6]
HTL - product HX	2013	0.7	2.2	[6]
HTL reactor	2013	1	2	[33]
Solid Filter	2011	0.6	1.7	[33]
CHG - Product HX	2013	0.7	2.2	[6]
Phase Separator	2011	0.68	1.9	[6]
Reformer	2007	0.65	1.92	[6]
PSA	2004	0.8	2.47	[6]
H2-compressor	2011	0.8	1.1	[6]
Steam Turbine	2010	0.85	1.08	[6]
HTL oil- storage	2005	0.65	2.95	[6]

**Table 3.4-2.** Cost factors for estimating the direct and indirect costs.

<b>Direct costs</b>	<b>Description</b>	<b>% of installed cost</b>
<b>Installed costs</b>		<b>100%</b>
Buildings	Necessary buildings required to operate day to day operations, such as warehouse, office etc.	1 %
Site development	Fencing, roads, parking lots, drainage etc.	9%
Additional piping	To connect the external utilities supply and demand with the plant facility.	4.5%
<b>Indirect costs</b>		<b>% of direct cost</b>
Prorated costs	This includes fringe benefits, burdens, and insurance of the construction contractor.	10%
Field expenses	Consumables, small tool and equipment rental, field services, temporary construction facilities, and field construction supervision.	10%
Home office and construction	Engineering plus incidentals, purchasing, and construction.	20%
Project contingency	Extra cash on hand for unforeseen issues during construction.	10%
Other costs	Startup and permits, other costs such as minor damages and additional labor requirement etc.	10%

**Table 3.4-3.** Material costs for the chemical and raw materials used for H<sub>2</sub>- production

Material	Category	Units	Unit price	Ref.
Macroalgae (Saccharina Japonica)	Raw Material	kg/hr	0.068	[15]
Water ( Process Water )	Raw material	kg/hr	0.00007	[6]
Natural Gas	Utility	kg/hr	0.56	[6]
HP-steam	Utility	kg/hr	0.02997	[32]
Cooling Utility (Cooling Water)	Utility	Gj/hr	0.354	[32]
Water makeup (Steam generation)	Utility	MT/hr	0.22	[32]
Power	Utility	kW	0.06	[32]
PSA Catalyst	Raw material	kg/hr	0.0036	[6]
Waste water treatment	Waste	gal/hr	0.0025	[32]
Solid Waste	Waste	kg/hr	0.36	[32]
Flue gas (Carbon Tax)	Waste	kg/hr	0.02	[34]
Net Power	Product	kW	0.0689	[32]
Net HP-steam	Product	kW	0.02929	[32]
Hydrogen	Product	kg/hr	6	[40]

## CHAPTER IV

### 4 COMBINED HEAT, HYDROGEN AND POWER PRODUCTION

#### 4.1. Process design and analysis

##### 4.1.1. Base case design

The process starts by taking the raw macroalgae as a feed. It is assumed that the raw feed contains 85% of moisture. Considering this assumption, the additional water required is mixed with the raw macro algae in a mixer. Prior to that the feed is crushed into size ranging from 1-3mm. Crushed *Saccharina japonica* is mixed with the water to maintain a ratio of 1:10 (why 1:10, will be explained in the section 5, based on the experimental results). Additional water when added, the slurry is then pumped to the reactor. Feed is pre-heated to a reaction temperature of 300 °C. The heating requirements for the heating section is met by a natural gas combustor. The hot flue gases raise the temperature of feed to reaction temperature. HTL reactor converts the solid biomass into liquid, gas and solids. The liquid fraction of the HTL product has 2 different phases, bio-oil (organic phase) and water-soluble organics (WSO). Solids from the HTL product are separated prior to phase separation of the gas and liquid. Gaseous product is removed by depressurizing. Liquid product is cooled down and two liquid phases are separated via gravity using a decanter. Here, two liquids are termed as the bio-oil (major organics) and the WSO (major fraction of water with dissolved organics).

The separated product from the HTL is then ready to be sent to the reforming unit. Before that, the liquid product is re-pressurized and heated. Similarly, the flashed gas is compressed and then sent to the pre-heater of the reforming section, where it gets pre-heated by the hot flue gases coming from the combustor at 600 °C. The circulation of natural gas is kept enough to keep flue gases hot enough to provide heating requirements till steam reformer section. Steam requirements for the SRU are met by purchasing steam externally. Addition of steam ensure better conversion into CO<sub>2</sub> and CH<sub>4</sub>. Steam reforming utilizes HP-steam to breakdown methane into CO and H<sub>2</sub>. Steam reforming takes place at a temperature of 850 °C at a pressure of 25 atm. The feed is breakdown into CO<sub>2</sub>, H<sub>2</sub>, CO and other minute gases. High temperature (HTS) converts this CO and H<sub>2</sub> further into excessive H<sub>2</sub> and CO<sub>2</sub>. 2-stage water gas shift conversion ensure better conversion of CO into CO<sub>2</sub> and H<sub>2</sub> in the presence of water. Later the HTS product is cooled down to lower temperatures of 40°C, compressed and send to the pressure adsorption unit. Here, H<sub>2</sub> is separated from the other impurities and is delivered at higher pressures. A part of H<sub>2</sub> is recycled back to ensure purity of H<sub>2</sub>. Power requirements for all the sections are met by purchasing electricity externally. Figure 4.1-1 shows the block diagram for the base case.

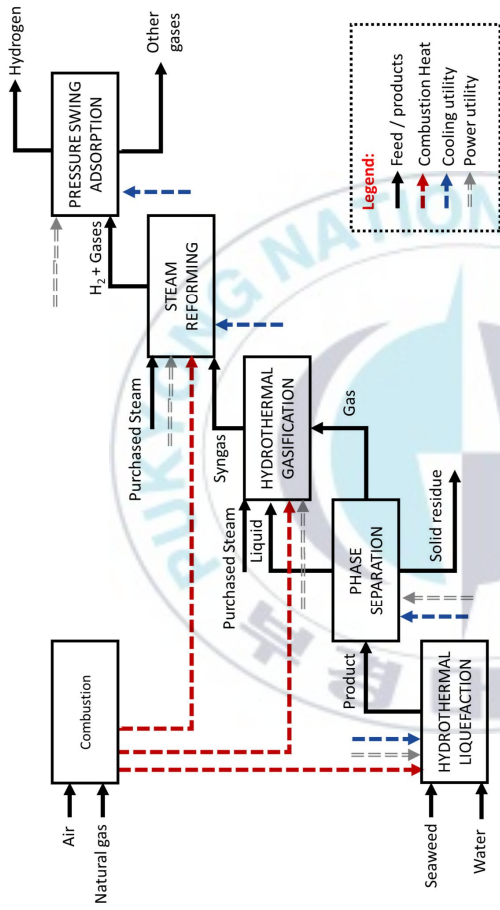


**Figure 4.1-1.** Block diagram for the base case design, which incorporates the combustor unit, which provides heating requirements for all the process sections.

## 4.2. Design alternatives

### 4.2.1. Case 1

With consideration to the base case design, keeping in view the high heating requirements for the design. The design was modified by making appropriate changes by incorporating the heat-integration system and on-site steam and power production. The main concerns in the base case design were the utilization of high amount of natural gas. With our claim that, we will reduce the use of fossil fuels, if we use high amount of natural gas, the claim won't have enough credibility. Therefore, the design was modified by introducing heat integrations and hot-oil system for the heating of the HTL feed. This design also incorporated a fired heater running on natural gas to provide heating requirements for the system, but the demand for natural gas was reduced by using hot streams to raise the temperature for the cold streams and hot-oil. Hot-oil system was used to provide heating requirements for the HTL section. HTL-oil was pre-heated via the hot HTL product. Finally, temperature was raised to 305 °C via flue gases coming from the fired heater which was running on the natural gas. Hot product coming from the HTL reactor was first sent to a separator where solids were separated. Later, hot HTL product was used to pre-heat the hot oil which was going to be later used as a heating medium for the HTL feed. Hot-oil was raised to its final temperature of 300°C via flue gases coming from the fired heater. Hot HTL product after pre-heating the hot-oil then further exchanges heat with the HTL feed. It pre-heats the HTL feed to a temperature of 105 °C and the hot HTL product leaves at a temperature of 66°C, relatively cool for the phase separation. Prior to the HTL feed preheating, the HTL feed is preheated to a temperature of 52 °C via the hot

stream exiting the HTS section. Prior to PSA, the stream needs to be at a cooler temperature. So, the temperature of the HTS stream is lowered via heat exchange with the HTL feed and via LT-steam production. Hot-oil keeps in circulation and exits at a temperature of 120 °C after heating the HTL final reactor feed to a temperature of 300 °C. Additional three heat exchangers were employed to raise the feed temperature and lower the HTL product temperature to significant extent of 105 °C and 66 °C respectively. Product leaving the HTL section then goes for phase separation where gases is flashed via depressurizing, and the 2 liquid phases are separated via a decanter. Waste water is removed, and the liquid and gas phase is again pressurized at a pressure of 25 atm. This stream is then pre-heated to a temperature of 600 °C via the hot flue gases coming from the fired heater after heating the hot-oil to a temperature of 305 °C. the flue gases pre-heats the reformer feed to a temperature of 600 °C. The hot flue gases with its remaining heat content is utilized to produce HP-steam for the SRU unit. after HP-steam, the flue gases are vent at a temperature of 120 °C. Feed then enters the pre-reformer, which is a part of reformer, where the feed is broken down into gases like CO, CO<sub>2</sub>, H<sub>2</sub> etc. pre-reformer product, is then heated to a temperature of 850 °C via a fired heater. Flue gases from combustor after maintain reformer feed temperature at 850 °C then keep the vapor fraction of the HP-steam for power generation to 1, in order to avoid damage in the turbine and is then vent at a temperature of 120 °C. Reformer product is cooled down via HP-steam production at a pressure of 125 bars. This HP-steam is then used for the power generation. The SRU product then entered the HTS unit. As we know, water gas shift reaction is an endothermic process, therefore, temperature raise in this section are

employed to produce LP-steam as a product. HP-steam generated from the HTS product produces a total power of 21.5 MW. Total system requirement for power are 3.6 MW. Thus, a net power of 17.8 MW is available. Steam enters the steam turbine at a pressure of 125 bar. Steam turbine in this design operates at a discharge pressure of 1 atm. HTS product after generating LP-steam is then cooled to a temperature of 45 °C via heat exchange with the HTL feed. HTS-product is then further compressed and sent to PSA where H<sub>2</sub> is separated and 15 % of the H<sub>2</sub> stream is recycled to ensure high purity of H<sub>2</sub>. Figure 4.2-1. Case 1, with on-site steam generation and power production. this case incorporates the heat -integration to reduce the consumption of natural gas required for the heating requirements. illustrates the design overview for the case 1.

#### 4.2.2. Case 2

Another alternative for the case 1 was proposed. This case considers that if the heating requirements are met by combusting a fraction of HTL liquid (bio-oil and WSO). With the fact that utilizing the liquid fraction for combusting would decrease the hydrogen production eventually but would be promising as it would eliminate the reliance on external utilities especially natural gas. The feasibility for this case was further evaluated by studying its economics in the later sections of the thesis. Figure 4.2-2. Proposed design for case 2, incorporating liquid product as a combustion fuel for providing heating requirements for the system. shows the schematic of the proposed design for the case 3.

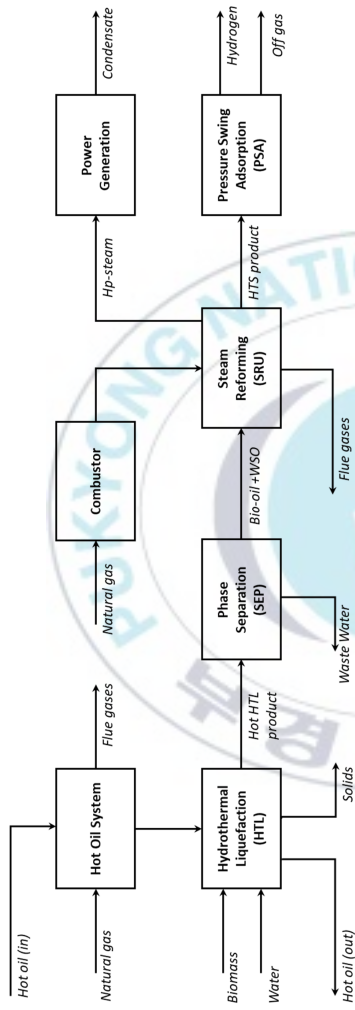


**Figure 4.2-1.** Case 1, with on-site steam generation and power production. this case incorporates the heat - integration to reduce the consumption of natural gas required for the heating requirements.

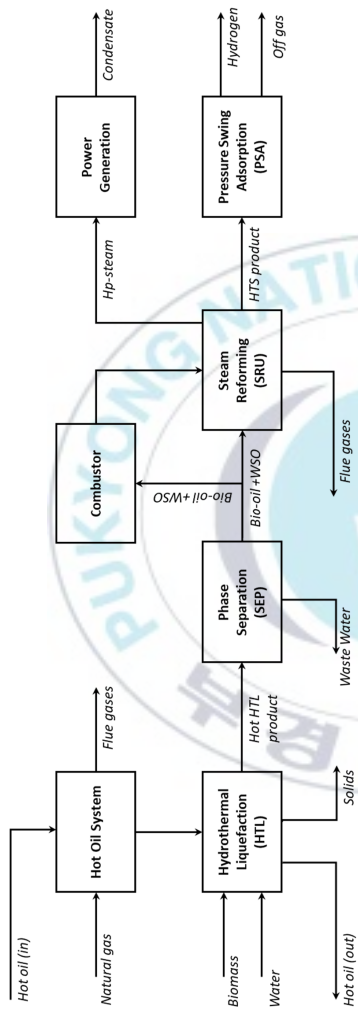


**Figure 4.2-2.** Proposed design for case 2, incorporating liquid product as a combustion fuel for providing heating requirements for the system.

### 4.3. Process description

#### 4.3.1. Hydrothermal liquefaction

The feed (biomass and water) is pumped at a pressure of 84 bars. HTL reactor is operating at a temperature of 300 °C. The operating conditions selected are based on the experimental results which will be mentioned in the later section. The HTL is modelled using 480,000 ton/year of *Saccharina japonica* as a feed and SRK-KD (SRK-kabaddi Danner) as a property method for HTL. This specific model can handle the organic and the water-based systems. Raw *Saccharina japonica* (85% moisture) is mixed with additional water to ensure the biomass to water ration of 1:10. For base case, HTL reactor heating requirements are supported by a combustor whereas in case 1 and case 2 HTL reactor heating requirements are supported by hot oil system in-directly heated by a fired heater running on natural gas. Hot-oil system was used to provide heating requirements for the HTL section. HTL-oil was pre-heated via the hot HTL product. Finally, temperature was raised to 305 °C via flue gases coming from the fired heater which was running on the natural gas. Hot product coming from the HTL reactor was first sent to a separator where solids were separated. Later, hot HTL product was used to pre-heat the hot oil which was going to be later used as a heating medium for the HTL feed. Hot-oil was raised to its final temperature of 300°C via flue gases coming from the fired heater. Hot HTL product after pre-heating the hot-oil then further exchanges heat with the HTL feed. It pre-heats the HTL feed to a temperature of 105 °C and the hot HTL product leaves at a temperature of 66°C, relatively cool for the phase separation. Prior to the HTL feed preheating, the HTL feed is preheated to a temperature of 52 °C via the hot stream exiting

the HTS section. Prior to PSA, the stream needs to be at a cooler temperature. So, the temperature of the HTS stream is lowered via heat exchange with the HTL feed and via LT-steam production. Hot-oil keeps in circulation and exits at a temperature of 120 °C after heating the HTL final reactor feed to a temperature of 300 °C. Additional three heat exchangers were employed to raise the feed temperature and lower the HTL product temperature to significant extent of 105 °C and 66 °C respectively. Product leaving the HTL section then goes for phase separation.



#### 4.3.2. Phase Separation

Reducer drops the HTL hot product pressure from 86 bars to 1 atm. Pressure is reduced to atmospheric pressure before phase separation for better separation. Flashed gases are compressed to a pressure of 25 atm. Free water is separated from the remaining HTL product mixture ( WSO, bio-oil and water) via decanter. WSO and bio-oil are sent to the pumps where they are re-pressurized. Hot flue gases in the HTL section generated from the fired heater for heating hot-oil are now used to pre-heat the liquid and gases to pre-reforming temperature of 600 °C. the hot flue gases raise their temperature to 600 °C and exit at a temperature of 672 °C. Still the gases are at a relatively higher temperature. These hot flue gases are then used to generate the HP-steam for the SRU unit. a total steam requirement for the SRU is calculated to be 124637 kg/hr. For case 2, the steam required for SRU is decreased due to the lesser amount of bio-oil to be reformed for the H<sub>2</sub> production. As a part of bio-oil is being used as a fuel for the SRU fired heater to provide heating requirements for the SRU unit. the amount of HP-steam used for the case 2 is 99452 kg/hr.

#### 4.3.3. Steam reforming unit

R-Gibbs reactor is employed for SRU. It is operated at a pressure of 25 bars and a temperature of 850°C with restricted chemical equilibrium and specified reaction conditions. The specified reaction ( $\text{CH}_4 + \text{H}_2\text{O} \rightarrow 3\text{H}_2 + \text{CO}$ ) converts the syngas methane into H<sub>2</sub> and CO. and lower hydrocarbons (C<sub>2</sub>-C<sub>4</sub>) . The steam reforming section converts HTL product into syngas by mixing the organics with the HP- steam. For base case and

case 1, additional heat required for SRU is provided by combustor flue gases which runs on natural gas. The flow rate of natural gas is adjusted to keep the outlet temperature of the reformer to 850°C. Reformer product is used to generate HP-steam. 80,000 kg/hr of HP-steam produced here is used for the power generation. Relatively cooled product is then sent to the HTS unit. In the design, WGS reaction – high temperature (300°C) shift (HTS) is employed to achieve maximum conversion of the CO [41]. Equilibrium reactor is used to model the WGS with specified reaction ( $\text{CO} + \text{H}_2\text{O} \rightarrow \text{CO}_2 + \text{H}_2$ ). The process of conversion of the CO to  $\text{CO}_2$  and  $\text{H}_2$  is endothermic due to which the product stream has a higher temperature. The increase in temperature is reduced by generating LP-steam. This LP-steam is used as a product. Still temperature need to be dropped further for the PSA section. This HTS-stream then exchanges heat with the HTL feed to pre-heat the feed to a temperature of 52 °C and leaves the HTL section at a temperature of 45 °C. The cooled product from then goes to the last section for  $\text{H}_2$  purification, where the product is cleansed from the impurities.

#### **4.3.4. Pressure swing adsorption (PSA)**

$\text{H}_2$  content is increased after coming from the LTS section. At this stage  $\text{H}_2$  is impure due to other impurities mainly  $\text{CO}_2$ , CO etc. The LTS product is cooled down to a temperature of 40°C by generating LP-steam. For Case 1, WGS product was cooled via cooling utilities purchases externally. For Case 2 and Case 3, the cooled product is flashed to remove the water from the product. The vapors are then compressed to a pressure of 27 bars and sent to the PSA unit. The separator separates the  $\text{H}_2$  from other gases. 85 % of

the hydrogen is recovered as a pure H<sub>2</sub> stream. Remaining 15% of the stream is recycled to increase H<sub>2</sub> purity.

#### **4.3.5. Steam turbine and power generation**

Steam turbine (ST) utilizes the HP-steam generated from the SRU hot product to generate power enough for the systems requirement. Moreover, the ST produces surplus power as a product, which can be used as a product to enhance the process economics. Power produced from this section thus meets the systems power requirements by every section. Steam turbine operates at a discharge pressure of 1 atm and generates a total power of 17.8 MW.

#### **4.4. Problem statement**

Based on high utility consumption with reference to H<sub>2</sub> production for the base case scenario. To make the technology feasible for industrial application, the process must be economically sound. Two different design cases are proposed to evaluate the process economics and to check which process yields the minimum hydrogen selling price (MHSP). To better understand the contribution for each case towards the economics and feasibility of the process, economic evaluation is performed for each case. Based on the techno-economic evaluation, results and conclusion will be drawn and an optimal pathway for H<sub>2</sub> will be chosen via HTL of *Saccharina japonica*.

## CHAPTER V

### 5 RESULTS AND DISCUSSION

#### 5.1. Experiments

##### 5.1.1. Characteristics of macroalgae

Dry macroalgae was used to study the reaction activity. Macroalgae *Saccharina japonica* was characterized via various analysis. These analyses include proximate analysis and ultimate analysis. ICP analysis was also performed to analyze the mineral contents for the biomass. The results for the characterization of dry macroalgae are reported in Table 5.1-1. Results included in this section was a collaborative effort with a PhD student, Yong Beom Park at a neighboring lab [42].

**Table 5.1-1.** Characterization of macroalgae with ultimate, proximate and ICP analysis.

Compositions	Macroalgae	Units
	Proximate analysis a	
Moisture	10.42	
Volatile matter	53.42	
Fixed carbon	5.28	Wt.%. (dry)
Ash	30.88	
	Ultimate analysis	
C	20.21	
H	3.23	
N	0.30	Wt.%. (dry)
S	1.11	
O	75.15	
	Minerals	
Na	31,370	
K	125,078	
Ca	31,747	mg/kg
Mg	6,287	

<sup>a</sup> Determined according to the ASTM E 1755 and 1756 standard method.

### 5.1.2. Effect of temperature

To evaluate the effect of temperature on the liquefaction conversion, reaction activity was studied for the course of various temperatures. The studying temperature varied from 180-300°C with an interval of 40°C for every experiment. For varying temperatures, initial set conditions for the residence time and the biomass: water ration was kept same as 2 hr and 1:10 respectively. In terms of appearance of the liquefaction liquid, the color tend to change with increasing reaction temperature. Liquefaction liquid tend to have a dark brown color up till 260 °C and changed to brown at a temperature of 300°C. The darkness in the color can be a reason for high amount of ash in the liquid. Solid residue was larger in size for lower temperatures and was blacker in color and smaller in size with increase in temperature. Table 5.1-2 shows the variations in color and size of solid residue. The autogenous pressure variations for the course of experiment were also recorded. With increase in reaction temperature from 180 to 300 °C, the pressure showed an increase from 9.2 to 84.4 bars respectively. Details for the pressures for individual temperature conditions are shown in the Table 5.1-3.

After reaction, the weight conversion were also observed. With increase in temperature from 180 to 300 °C , there was an increase in the liquefaction conversion from 70.0 to 91.0 %. Owing to maximum conversion of 91.0 %, 300°C was chosen as an optimal temperature for the HTL reaction. The carbon conversion of the product showed an increase with increasing temperature. Mineral contents also increased in the liquefied oil

with increase in temperature. A summary for the product yields with temperature variation is shown in Table 5.1-4

It was observed that with increasing temperature, the carbon conversion was also increased. On analyzing the liquid product for minerals, it was seen that minerals tend to be more soluble in the water, which was used as a solvent with increasing temperature. That's the reason behind high ash content in the liquefied oil. Results for the carbon conversion in the liquefied oil and solid residue along with mineral content in the liquefied oil and solid residue is shown in Table 5.1-5. Comparison for the liquefaction conversion on carbon basis and ash content for hydrothermal liquefaction for various temperatures is shown in the Figure 5.1-1 and Figure 5.1-2.

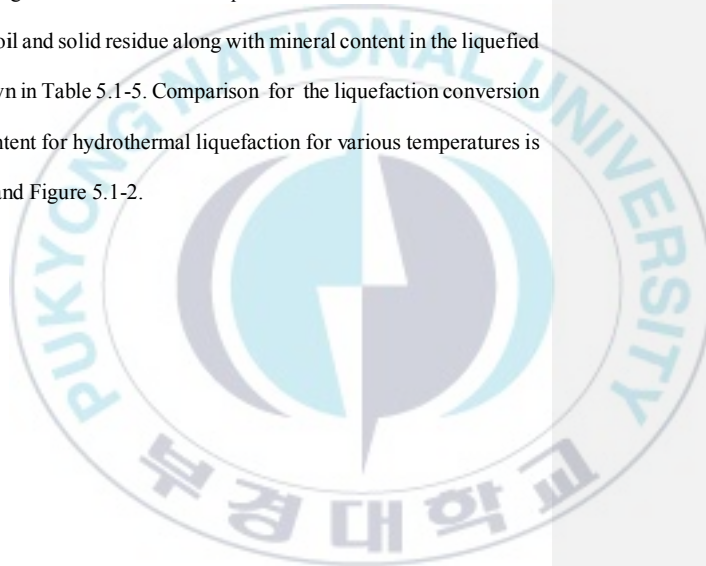


**Table 5.1-2.** Appearance of liquefaction liquid and solid residue with increasing temperature and at same residence time and feed: water ration.

No.	#1	#2	#3	#4
Condition	1/10 w/w, 180 °C, 2 hr	1/10 w/w, 220 °C, 2 hr	1/10 w/w, 260 °C, 2 hr	1/10 w/w, 300 °C, 2 hr
Liquid				
Residue				

**Table 5.1-3.** Effect of reaction temperature on experimental conditions.

No.	Particle size (mm)	Macroalgae/ H <sub>2</sub> O ratio (w/w)	Temp. (°C)	Time (hr.)	Pressure (bar)
1	1-3	1 / 10	180	2	9.2
2			220		22.5
3			260		45.4
4			300		84.4

**Table 5.1-4.** Product yields and liquefaction conversion with increasing temperature and fixed reaction time and macroalgae: water ratio of 2 hrs. and 1:10 respectively.

Temp. (C)	Liquefaction conversion (%)	Product yield (wt.%)		
		Liquid	Residue	Gas <sup>a</sup>
180	70.0	67.7	30	2.3
220	79.6	76.5	20.4	3.1
260	89.4	86.4	10.6	3
300	90.9	88.0	9.1	2.9

<sup>a</sup> Calculated by difference

**Table 5.1-5.** Effect of temperature on carbon conversion in the liquefied oil and solid residue along with mineral content in the liquefied oil and solid residue.

No.	Temp. (K)	Carbon content (wt.%)		ICP analysis (ppm)							
		Liquefied oil	Residue	Liquefied oil				Residue			
		C	C	Na	K	Ca	Mg	Na	K	Ca	Mg
1.	180	2.26	30.03	2274	5743	1392	50	84250	172527	70025	16675
2.	220	2.58	32.42	2682	6036	1593	987	104128	201557	100221	20332
3.	260	3.07	46.31	3052	6725	1732	1058	169754	270598	180021	68521
4.	300	3.42	53.64	3442	7052	1804	1147	178154	284459	179845	74236

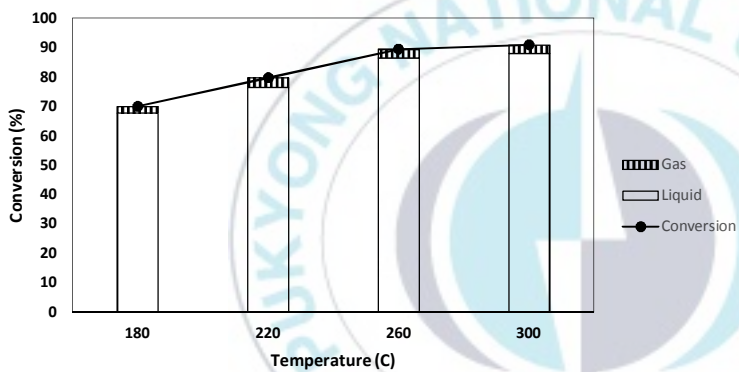


**Figure 5.1-1.** Effect of reaction temperature of conversion for hydrothermal liquefaction. (Conditions: Feed / H<sub>2</sub>O ratio=1 / 10, Time=2 h)

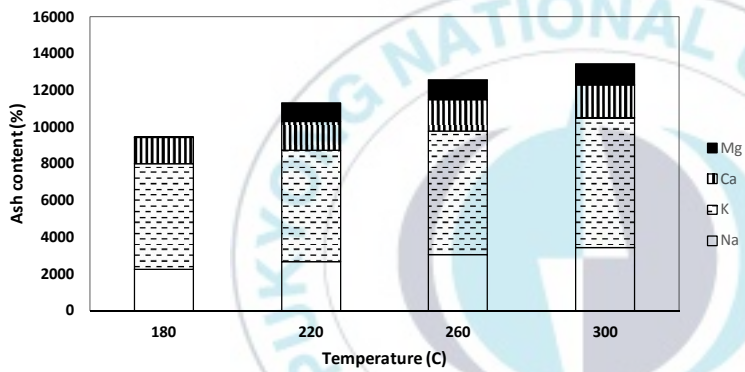


**Figure 5.1-2.** Effect of reaction temperature of ash content for hydrothermal liquefaction. (Conditions: Feed / H<sub>2</sub>O ratio=1 / 10, Time=2 h)

## 5.2. Effect of reaction time

HTL reaction activity was studied for a reaction time of 1, 2, and 4hrs. Based on the results from previous sections for the effect of temperature on the HTL reaction, further experiments were performed to evaluate the optimal time required for highest conversion. To evaluate the effect of time, reaction temperature of 300 °C and biomass: water was taken as 1:10.

With an increase in reaction time, increase conversion was observed from 90.7 to 91.0 %. For reaction time of 2 hrs. and 4hrs. there was a constant conversion. Since, higher reaction time would lead to higher energy costs. Reaction time of 1hr. was chosen as an optimal choice. Furthermore, reason behind choosing 1hr. of residence time reflects the fact that increased time would lead to increase in solubility for the minerals in the liquefied oil, which on later stages would affect the deactivation of the catalyst. Ash conversion was increased from 78.2 to 87.4%. Effect of reaction time on HTL activity is shown in Table 5.2-1.

Keeping in consideration the high amount of ash in the oil, despite higher carbon content conversion at higher reaction times, increase ash content in the liquefied oil was unfavorable. An increasing trend was observed for the carbon content of the liquefied oil. .

Effect of reaction time on conversion for hydrothermal liquefaction (Conditions: biomass / H<sub>2</sub>O ratio=1 / 10, Temperature= 300 °C) is shown in Figure 5.2-1 and Figure 5.2-2.

Effect of reaction time on liquefied oil carbon conversion and ash content for HTL at biomass: water ratio of 1:10 and reaction temperature of 300 °C is shown in Table 5.2-2.



**Table 5.2-1.** Product yields liquefaction conversion with increasing reaction time and fixed reaction temperature and macroalgae: water ratio of 300 °C and 1:10 respectively.

Time (hr.)	Pressure (bar)	Liquefaction conversion (%)	Product yield (wt.%)		
			Liquid	Residue	Gas
1	82.8	90.7	90.6	9.3	0.1
2	84.4	91.0	88.0	9.0	3.0
4	83.2	90.4	87.6	9.6	2.8

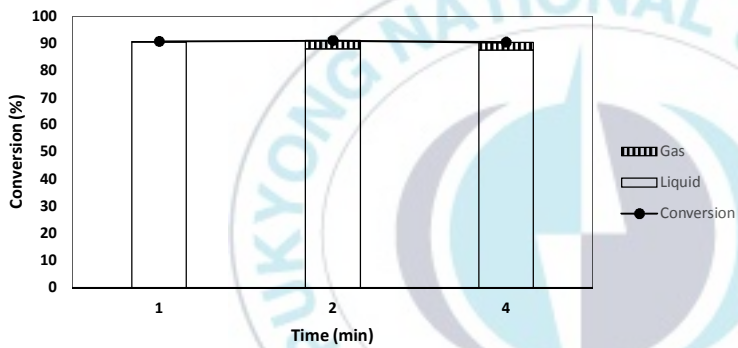


**Figure 5.2-1.** Effect of reaction time of conversion for hydrothermal liquefaction.  
 (Conditions: biomass / H<sub>2</sub>O ratio=1 / 10, Temperature= 300 °C)

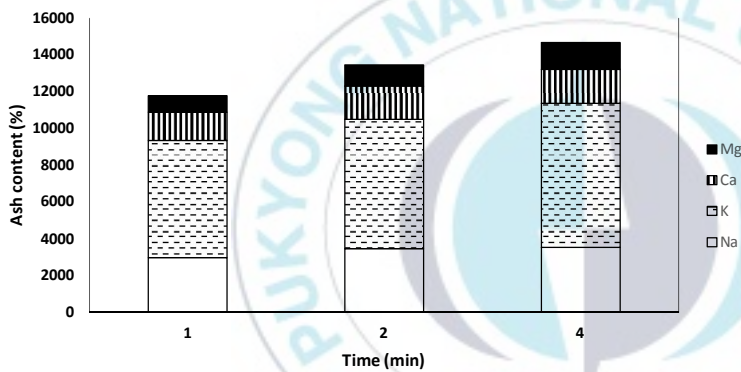


**Figure 5.2-2.** Effect of reaction time of ash content for hydrothermal liquefaction. (Conditions: biomass / H<sub>2</sub>O ratio=1 / 10, Temperature= 300 °C)

**Table 5.2-2.** Effect of reaction time on carbon conversion in the liquefied oil and solid residue along with mineral content in the liquefied oil and solid residue.

No.	Time (hr.)	Carbon content (wt.%)		ICP analysis (ppm)							
		Liquefied oil	Residue	Liquefied oil				Residue			
		C	C	Na	K	Ca	Mg	Na	K	Ca	Mg
1.	1	1.52	38.63	2972	6371	1542	872	107526	216548	120785	24556
2.	2	3.42	53.64	3442	7052	1804	1147	178154	284459	179845	74236
3.	4	3.50	51.77	3508	7854	1858	1433	134596	249275	116374	50223

### 5.2.1. Effect of biomass: water loading

For the effect of biomass to water ratio, we studied the effect of three different ratios on the HTL conversion. Biomass :water ratio included 1:5, 1:7 and 1:10. Based on conclusions from previous sections, our optimal temperature is 300 °C and the optimal reaction time is 1 hr. During the reaction , with optimal temperature and reaction time conditions, highest liquefaction conversion of 91.2 % was observed with 1/7 ratio. Following this 1/10 showed a liquefaction conversion of 91.0 %. Liu et al. reported that higher water content during reaction was more suitable for the conversion of organic compounds [31]. With water being the reaction medium, high temperatures of water with excess amount are generally suitable for the HTL reactions. Liquefaction conversion showed values of 77.5% to 91.0%, as the *Saccharina japonica*/H<sub>2</sub>O ratio decreased from 1/5 to 1/10. A minute difference of 0.21% was observed for macroalgae to water ratio of 1/7 and 1/10. Owing to the fact, high amount of water is favorable for HTL, so we selected 1/10 as an optimal macroalgae to water ratio. Table 5.2-3 shows the product yields and liquefaction conversion based on the biomass: water ratios. Effect of feed ratio on conversion for hydrothermal liquefaction is shown in Figure 5.2-3. Ash conversion for the liquefied oil is shown in Figure 5.2-4.

**Table 5.2-3.** Product yields and liquefaction conversion at varying biomass to water ratio at a temperature of 300 C and 1 hr. residence time.

No.	Biomass / H <sub>2</sub> O ratio (w/w)	Liquefaction conversion (%)	Product Yield (wt.%)		
			Liquid	Residue	Gas
1.	1 / 5	77.5	75.1	22.5	2.4
2.	1 / 7	91.2	88.4	8.8	2.8
3.	1 / 10	91.0	88.0	9.0	3.0

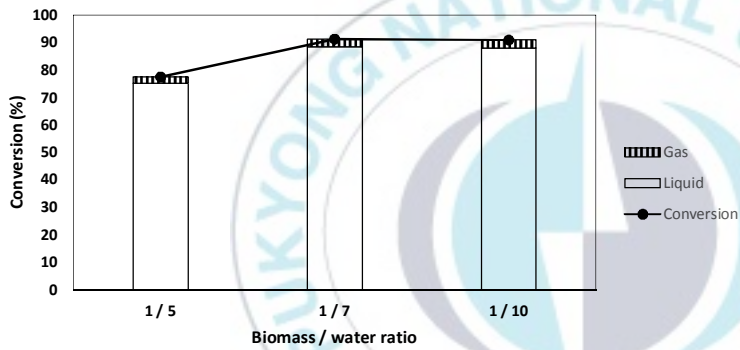


**Figure 5.2-3.** Effect of feed ratio of conversion for hydrothermal liquefaction.  
 (Conditions: Temperature=300 °C, Time=1 hr)

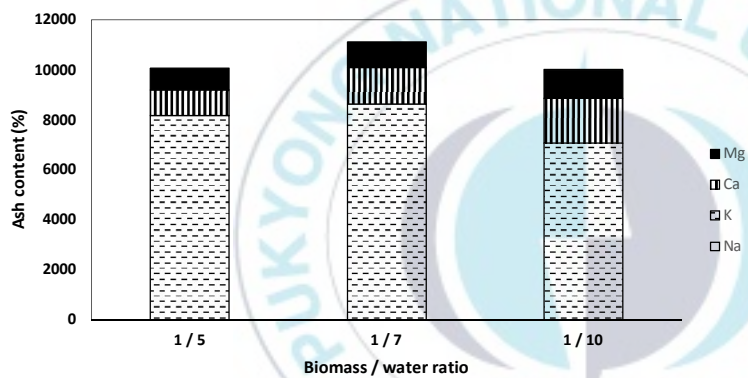


**Figure 5.2-4.** Effect of ash conversion for hydrothermal liquefaction. (Conditions: Temperature=300 °C, Time=1 hr)

### 5.2.2. HTL compound and group distribution

On studying the effect of various conditions, optimal conditions 300 °C temperature, 1 hr. of reaction time and 1/10 ratio of biomass to water were chosen as optimal conditions. To study the compound distribution for the liquid phase GC-MS analysis for the optimal conditions was performed. The liquid phase comprised of 2 phases 1- Bio-oil (organic phase) and 2- Water soluble organics (WSO, the aqueous phase). Both phases were collected separately as described in the separation schematic in the previous sections for separation of the product from the HTL product mixtures. GC-MS analysis for the liquid phases were performed to study the compound and group distributions. Table 5.2-4 and Table 5.2-5 shows the compound distribution of the bio-oil and the aqueous phase respectively. The main components in the liquefied oil were reported to be ketones, aldehydes, aromatics, heterocyclic, aliphatic and some nitrogen containing compounds. Ketones and aldehydes were found in abundance in comparison to other functional groups.

**Table 5.2-4.** Organic (bio-oil) compounds distribution for the HTL product liquid mixture at a reaction temperature of 300, 1hr residence time and 1/10 biomass to water ratio.

No.	Name of Compound	Area %	Time (min)
<b>Alcohol</b>			
1	1-Butanol, 2-methyl-	2.6	4.5
2	1-Butanol, 3-methyl-	1.9	6.7
<b>Ketone</b>			
3	Cyclopentanone	3.4	8.1
4	Cyclopentanone, 2-methyl-	0.8	9.7
5	2-Pentanone	0.7	10.2
6	2-Ethylidenecyclohexanone	4.2	14.8
7	3-Pentanone	1.5	11.1
8	Cyclohexanone, 3-ethenyl-	1.9	12.2
9	3-Hexanone	1.8	13.5
10	Cyclohexanone	2.0	12.8
11	2-Ethylidenecyclohexanone	4.1	9.7
<b>Aldehyde</b>			
12	Butanal, 2-methyl-Pentanal	2.7	5.6
13	2-Butenal, 2-ethenyl-	1.8	6.4
14	2-Cyclopenten-1-one, 2-methyl	1.9	6.9
15	2-Cyclopenten-1-one, 2,3-methyl	3.4	7.5
16	3,7,11-Trimethyl-2,4-dodecadiene	4.2	8.4
17	Hexadecane	5.1	14.2
<b>Hydrocarbons</b>			
18	2-Cyclopenten-1-one, 3-methyl	1.7	15.8
19	Cyclopropene	4.2	19.4
20	2-Cyclohexen-1-one, 4-ethyl-4-methyl-	1.8	13.4
21	1-Ethylcyclopentene	2.6	15.7
22	2-Cyclohexen-1-one, 4-(1-,methylethyl)-	2.8	17.2
<b>Nitrogen-containing</b>			
23	1H-Pyrrole, 1-methyl-Pyrrole	1.7	13.1
24	1H-Pyrrole, 1-butyl	4.5	24.1
25	1H-Pyrrole, 1-pentyl	2.2	22.5
26	1,3-Diazine	3.1	18.7
27	Indolizine	5.5	12.3
28	Indole, 3-methyl-	4.9	11.8

\*Using ethanol solvent for analysis

**Table 5.2-5.** Aqueous phase compounds distribution for the HTL product liquid mixture at a reaction temperature of 300, 1hr residence time and 1/10 biomass to water ratio.

No.	Name of Compound	Area %	Time (min)
<b>Alcohol</b>			
1	1-Butanol, 2-methyl-	2.4	4.6
<b>Ketone</b>			
2	Cyclopentanone	1.1	8.0
3	Cyclopentanone, 2-methyl-	0.7	9.7
4	Cyclopentanone, 2-ethyl-	4.1	10.5
5	2-Ethylidenecyclohexanone	3.5	14.8
6	3-Ethylcyclopentanone	1.2	13.9
7	2-Butanone, 3-methyl-	0.8	6.7
8	3-Hexanone	1.4	5.2
9	2-Hexanone	2.7	6.0
<b>Aldehyde</b>			
10	Butanal, 2-methyl-Pentanal	1.9	5.6
11	2-Butenal, 2-ethenyl-	1.5	6.4
12	2,2-Dimethylocta-3,4-dienal	2.9	25.2
<b>Heterocyclic</b>			
13	Furan, 2,5-dimethyl-	0.5	21.2
14	2,4-Dimethylfuran	1.7	22.3
15	Furan, 2-ethyl-	0.4	24.1
16	Furan, 2,3,5-trimethyl-	1.1	23.8
<b>Aromatics</b>			
17	2-Methoxy-5-methylphenol	0.9	19.9
<b>Hydrocarbons</b>			
18	2-Cyclopenten-1-one, 2-methyl	1.8	15.7
19	2-Cyclopenten-1-one, 2,3-dimethyl-	1.7	16.2
20	3,7,11-Trimethyl-2,4-dodecadiene	2.4	8.4
21	3-Octyne, 7-methyl-	2.6	17.2
22	Cyclopropene	3.8	19.4
23	4,4-Dimethyl-2-cyclopente-1-one	4.0	20.0
24	Cyclohexene	1.4	17.6
25	3,5-Dimethylcyclopentene	1.7	15.2
<b>Nitrogen-containing</b>			
26	9-Octadecenamide	0.9	19.2
27	1,3-Diazine	3.7	18.7
28	Indolizine	2.5	12.3
29	Indole, 3-methyl-	4.1	11.8
30	1H-Pyrrole, 2,3,5-trimethyl-	3.0	10.9

31	Piperidine, 1-ethyl-	4.1	9.2
32	1,2,5-Trimethylpyrrole	0.9	8.5
33	1H-Pyrrole, 2,4-dimethyl-	0.8	9.4
34	2-Methyl-3-propylpyrazine	1.7	13.2
35	2-Isobutyl-3-methylpyrazine	1.1	12.8
36	3-Pyridinol, 2-methyl	1.3	12.5

\*Using ethanol solvent for analysis



### 5.2.3. Summary of activity of HTL via macroalgae

With increase in reaction temperature, carbon content was increased from 1.52 to 3.50 % and S/C ratio was decreased from 22.4 to 15.4. Carbon content had an increasing trend when macroalgae: water was increased, and S/C ratio was decreased from 26.4 to 15.8. The effect of the reaction time was examined and as the reaction time was increased, the carbon content was increased from 1.52 to 3.50 wt.%, while S/C ratio was reduced from 22.4 to 15.4. S/C ratio for HTL for macroalgae was much higher than the terrestrial biomass, which is in a range of 6-8 [31]. The effect of the reaction time was examined and as the reaction time was increased, the carbon content was increased from 1.52 to 3.50 wt.%, while S/C ratio was reduced from 22.4 to 15.4.

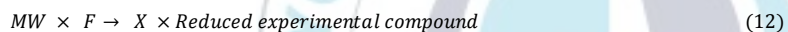
## 5.3. Simulation results

### 5.3.1. Process modelling

Table 5.2-4 and Table 5.2-5 shows the list of experimental compounds detected in the liquid. While using a process simulator, a greater number of compounds lead to longer iterative time taken by process simulators. In-order to deal with this, recently developed automated bio-crude reduction software was employed for reduction of the experimental compounds. The method requires basic input data which includes feed's ultimate and proximate analysis, HTL product phase distribution, GC-MS spectra for the bio-oil and WSO, and composition for solid residue and gas [35]. Complex liquid mixtures (bio-oil and WSO) containing numerous compounds are reduced to a number which can save iterative time taken by process simulator. Compound reduction is performed keeping

weighted average molecular mass and boiling point differences between the original compounds and the reduced compounds as a constraint. The software provides with a ready to use reduced mixture and in mass balance with the feed's ultimate and proximate analysis. Reduction results obtained after processing the experimental data are shown in Table 5.3-1. The software also provides with a graphical GC-MS spectrum for a comparison for the trends of cumulative normalized peak area vs the retention time for the original and the reduced mixture. Respective graphs are shown in Figure 5.3-1.

The software also provides a ready to input feed and reactor balanced data for the aspen plus stoichiometric reactor. Reactor input data for the stoichiometric reactor is represented by the equation (6).



where, MW, F, and X denote molecular weight of the experimental compound, feed (biomass), and fractional conversion of the experimental compound, respectively. Ready to use reduced mixture along with fractional conversions based on the experimental data and CAS numbers are shown in Table 5.3-2.

**Table 5.3-1.** The stats of current experimental data run from the reduction software.

	<b>Organic Mixture</b>	<b>Aqueous Mixture</b>
No. of original compounds	28	36
No. of reduced Compounds	9	13
Reduction Factor	3.11	2.77

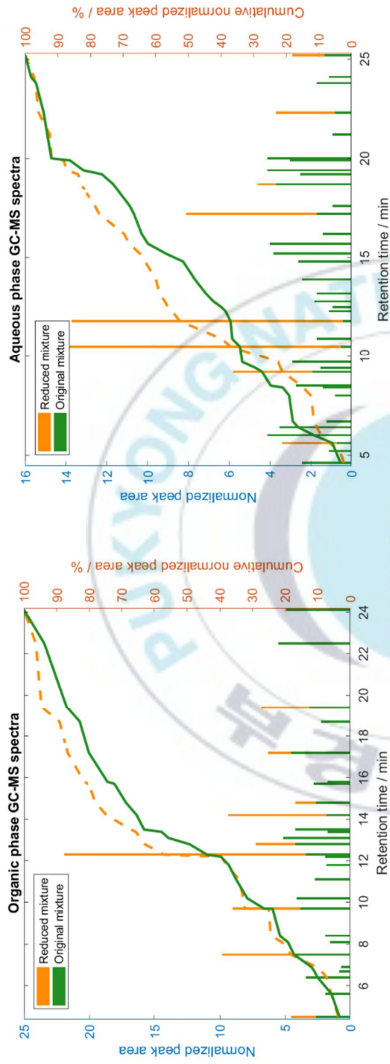


**Figure 5.3-1.** GC-MS spectra of the original mixture and the reduced mixture for the organic phase (bio-oil) and the water-soluble phase (Aqueous Phase).

**Table 5.3-2.** Ready to use reduced mixture along with fractional conversions.

No.	Name	Chemical Formula	CAS Number	Fractional Conv.
1	1-Butanol, 2-methyl-	C5H12O	137-32-6	0.015361
2	2-Ethylidenecyclohexanone	C8H10O	90-00-6	0.022449
3	Cyclohexanone	C6H10O	108-94-1	0.017959
4	2-Ethylidenecyclohexanone	C8H14	764-13-6	0.010476
5	Hexadecane	C16H34	544-76-3	0.023197
6	2-Cyclopenten-1-one, 2,3-methyl	C7H9N	591-22-0	0.024445
7	Cyclopropane	C3H4	74-99-7	0.016962
8	2-Cyclohexen-1-one, 4-(1-methylethyl)-	C10H14	488-23-3	0.015664
9	Indolizine	C8H8O	104-87-0	0.054626
10	Cyclopentanone, 2-ethyl-	C7H12O	2043-61-0	0.026717
11	Butanal, 2-methyl-Pentanal	C8H12	694-92-8	0.005860
12	2,2-Dimethylocta-3,4-dienal	C10H15N	91-66-7	0.004999
13	2,4-Dimethylfuran	C6H10O	557-40-4	0.006378
14	2-Methoxy-5-methylphenol	C8H10O2	93-51-6	0.001551
15	3-Octyne, 7-methyl-	C9H18	4588-18-5	0.013962
16	2-Cyclopenten-1-one, 2-methyl	C6H10O	108-94-1	0.006033
17	Cyclopropene	C3H4	74-99-7	0.006550
18	4,4-Dimethyl-2-cyclopenten-1-one	C7H12O	2043-61-0	0.006895
19	Piperidine, 1-ethyl-	C8H16	2040-96-2	0.009997
20	Indole, 3-methyl-	C8H8O2	99-04-7	0.023614
21	1,3-Diazine	C4H4N2	289-95-2	0.007929
22	CO	CO	630-08-0	0.000051
23	CO2	CO2	124-38-9	0.000514
24	H2	H2	1333-74-0	0.000001
25	CH4	CH4	74-82-8	0.000008
26	C2H4	C2H4	74-84-0	0.000002
27	C2H6	C2H6	74-85-1	0.000006
28	C3H8	C3H8	74-98-6	0.000004
29	>C4 hydrocarbons	C4H10	> 106-97-8	0.000002
30	Water	H2O	7732-18-5	0.117927
31	Char	N/A	N/A	0.559859

### 5.3.2. Process stream flow description

While performing simulation via aspen plus, we can get the material and energy balance from the aspen. For better understanding, a complete layout for the Case 1 is shown in Figure 5.3-2. Complete process flow diagram for the combined heat, power and hydrogen production via HTL of *Saccharina japonica*. Major process stream summary and data inputs to the process sections is shown in Table 5.3-3. Starting with HTL section, an input of 60,000 kg/hr of *Saccharina japonica* is fed to the HTL reactor. HTL process temperature is kept at a temperature of 300 °C. For base case, HTL reactor heating requirements are supported by a combustor whereas in case 1 and case 2 HTL reactor heating requirements are supported by hot oil system in-directly heated by a fired heater running on natural gas. Hot-oil system was used to provide heating requirements for the HTL section. HTL-oil was pre-heated via the hot HTL product. Finally, temperature was raised to 305 °C via flue gases coming from the fired heater which was running on the natural gas. Hot product coming from the HTL reactor was first sent to a separator where solids were separated. Later, hot HTL product was used to pre-heat the hot oil which was going to be later used as a heating medium for the HTL feed. Hot-oil was raised to its final temperature of 300°C via flue gases coming from the fired heater. Hot HTL product after pre-heating the hot-oil then further exchanges heat with the HTL feed. It pre-heats the HTL feed to a temperature of 105 °C and the hot HTL product leaves at a temperature of 66°C, relatively cool for the phase separation. Prior to the HTL feed preheating, the HTL feed is preheated to a temperature of 52 °C via the hot stream exiting the HTS section. Prior to PSA, the stream needs to be at a cooler temperature. So, the temperature of the

HTS stream is lowered via heat exchange with the HTL feed and via LT-steam production. Hot-oil keeps in circulation and exits at a temperature of 120 °C after heating the HTL final reactor feed to a temperature of 300 °C. Additional three heat exchangers were employed to raise the feed temperature and lower the HTL product temperature to significant extent of 105 °C and 66 °C respectively. Product leaving the HTL section then goes for phase separation. Reducer drops the HTL hot product pressure from 86 bars to 1 atm. Pressure is reduced to atmospheric pressure before phase separation for better separation. Flashed gases are compressed to a pressure of 25 atm. Free water is separated from the remaining HTL product mixture ( WSO, bio-oil and water) via decanter. WSO and bio-oil are sent to the pumps where they are re-pressurized. Hot flue gases in the HTL section generated from the fired heater for heating hot-oil are now used to pre-heat the liquid and gases to pre-reforming temperature of 600 °C. the hot flue gases raise their temperature to 600 °C and exit at a temperature of 672 °C. Still the gases are at a relatively higher temperature. These hot flue gases are then used to generate the HP-steam for the SRU unit. a total steam requirement for the SRU is calculated to be 124637 kg/hr. For case 2, the steam required for SRU is decreased due to the lesser amount of bio-oil to be reformed for the H<sub>2</sub> production. As a part of bio-oil is being used as a fuel for the SRU fired heater to provide heating requirements for the SRU unit. the amount of HP-steam used for the case 2 is 99452 kg/hr. R-Gibbs reactor is employed for SRU. It is operated at a pressure of 25 bars and a temperature of 850°C with restricted chemical equilibrium and specified reaction conditions. The specified reaction ( $\text{CH}_4 + \text{H}_2\text{O} \rightarrow 3\text{H}_2 + \text{CO}$ ) converts the syngas methane into H<sub>2</sub> and CO. and lower hydrocarbons (C<sub>2</sub>-C<sub>4</sub>) . The steam

reforming section converts HTL product into syngas by mixing the organics with the HP-steam. For base case and case 1, additional heat required for SRU is provided by combustor flue gases which runs on natural gas. The flow rate of natural gas is adjusted to keep the outlet temperature of the reformer to 850°C. Reformer product is used to generate HP-steam. 80,000 kg/hr of HP-steam produced here is used for the power generation. Relatively cooled product is then sent to the HTS unit. In the design, WGS reaction – high temperature (300°C) shift (HTS) is employed to achieve maximum conversion of the CO [41]. Equilibrium reactor is used to model the WGS with specified reaction ( $\text{CO} + \text{H}_2\text{O} \rightarrow \text{CO}_2 + \text{H}_2$ ). The process of conversion of the CO to  $\text{CO}_2$  and  $\text{H}_2$  is endothermic due to which the product stream has a higher temperature. The increase in temperature is reduced by generating LP-steam. This LP-steam is used as a product. Still temperature need to be dropped further for the PSA section. This HTS-stream then exchanges heat with the HTL feed to pre-heat the feed to a temperature of 52 °C and leaves the HTL section at a temperature of 45 °C. The cooled product from then goes to the last section for  $\text{H}_2$  purification, where the product is cleansed from the impurities.  $\text{H}_2$  content is increased after coming from the LTS section. At this stage  $\text{H}_2$  is impure due to other impurities mainly  $\text{CO}_2$ , CO etc. The LTS product is cooled down to a temperature of 40°C by generating LP-steam. For Case 1, WGS product was cooled via cooling utilities purchases externally. For Case 2 and Case 3, the cooled product is flashed to remove the water from the product. The vapors are then compressed to a pressure of 27 bars and sent to the PSA unit. The separator separates the  $\text{H}_2$  from other gases. 85 % of the hydrogen is recovered as a pure  $\text{H}_2$  stream. Remaining 15% of the stream is recycled

to increase H<sub>2</sub> purity. Steam turbine (ST) utilizes the HP-steam generated from the SRU hot product to generate power enough for the systems requirement. Moreover, the ST produces surplus power as a product, which can be used as a product to enhance the process economics. Power produced from this section thus meets the systems power requirements by every section. Steam turbine operates at a discharge pressure of 1 atm and generates a total power of 17.8 MW.



**Table 5.3-3.** Summary for the major process input and reaction parameters for the process.

<b>Category</b>	<b>Value</b>
Saccharina Japonica (kg/hr) dry basis.	60,000
Water (Ton/hr)	600
<b>Hydrothermal Liquefaction</b>	
Temperature °C	300
Pressure (bar)	84
Liquefaction	88.78
Conversion (%)	
<b>Yields (wt.%)</b>	
Bio-oil	22.16
Aqueous Organics (WSO)	68.51
Gas <sup>a</sup>	0.057
Solid Residue	9.259
<b>Gas composition b (wt.%)</b>	
CO <sub>2</sub>	88.3
H <sub>2</sub>	0.9
CH <sub>4</sub>	1.8
CO	9
<b>Water Composition (wt.%)</b>	
Organic Phase Moisture	8.63
Aqueous Phase Moisture	84.52
<b>Steam Reforming</b>	
S/C Ratio	3.5

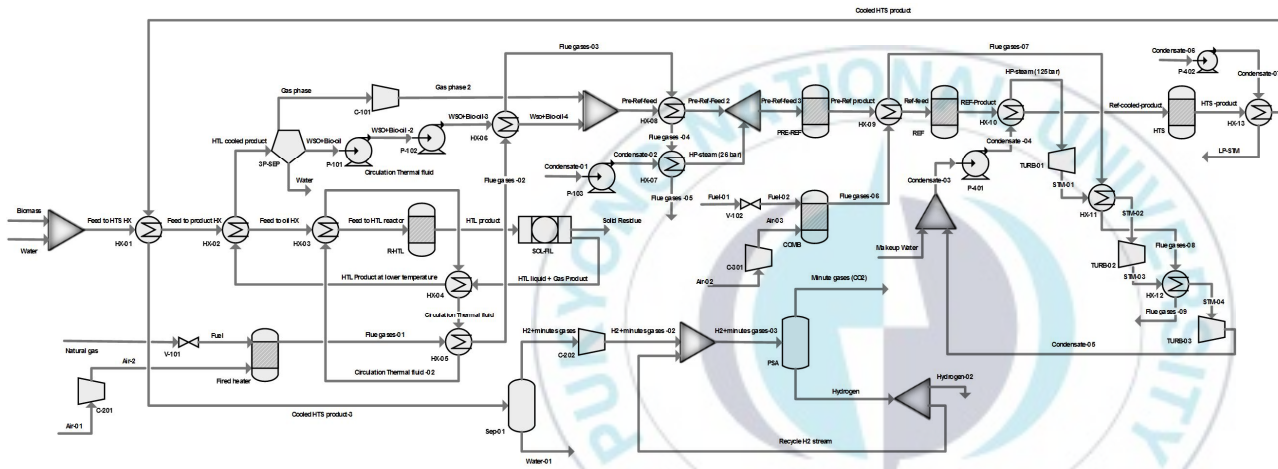


Figure 5.3-2. Complete process flow diagram for the combined heat, power and hydrogen production via HTL of *Saccharina japonica*.

### 5.3.3. Installation cost breakdown

The total costs for the equipment was calculated from literature study from various sources [6,37,38]. A part of the costs for the HTL and the HG unit were calculated based on the costs from the Aspen economic analyzer. There was not enough data in literature for the costing of the reactors and equipment's at autogenous pressure for our study. Most of the studies reported the costs based on high pressure of 20 MPa. Therefore, keeping in mind the parameters such as size, material of construction and pressure, the equipment cost was analyzed via CAPCOST and aspen plus cost estimator. The costs for the major sections included in the process simulation are shown in the Table 5.3-4.

As we can see in the Table 5.3-4 the equipment installation costs for each design varies depending upon the design. For the base case, there is no heat integration. Addition to that Base case includes no steam generation and power production so that also contributes to lesser cost. In comparison to design alternative, Case 1 had the highest cost for equipment installation. Case 1 also had the highest H<sub>2</sub> production rate. As for Case 2 we considered that, a part of the HTL product stream is going to be utilized as a combustion fuel, that reflects the lower equipment costs for Case 2. Costs for the equipment are calculated based on the capacity of the equipment. Cost factors and equipment flows are used to calculate the cost of equipment's. For Case 2, lesser stream flow in comparison to Case 1 for CHG and subsequent units due to splitting of the HTL product for combustion purposes owes for lesser cost. For Case 1 and Case 2, additional heat exchangers for heat integration, on-site steam and power production system adds up to

the costs for design alternatives. Based on these values, we are going to set up the technoeconomic model to assess the feasibility of each design case.

#### **5.3.4. Manufacturing costs**

Unit price for material stream were taken from literature studies [6,34,37–39]. Major material streams used in the simulation for techno-economic assessment is given in Table 5.3-5. Major cost contributors were the utilities for Base Case 1. 24834 kg/hr of natural gas required for combustion to support heating requirements incurred a total investment of 112 \$MM. Beside that for Base Case, HP-steam was purchased externally which added an additional cost of 32 \$MM. Based on these values, the costs for these utilities were lowered to a great extent by modifying the base case design by installing heat integration, on-site steam and power generation. A natural gas flow was reduced by 66 % by integrating the process sections. Costs for the process streams is shown in Table 5.3-6

De-ionized water was used for the steam production. HP-steam was generated for power production via steam turbine. Total power consumption by the pumps and compressors installed in the Base Case and the design cases differed slightly. Total power requirement for the Base Case was 3011 KW. Case 1 and Case 2 were designed in accordance to fulfill the power requirements for the Base Case. Case 1 and Case 2 generated a total power of 17.8 MW respectively. The produced power was enough to provide the plant demands. Reformer product 's high temperature was lowered for the HTS unit by generating high pressure steam. Further temperature was lowered via generating low-pressure steam and was considered as a product.

**Table 5.3-4.** Installation costs breakdown for the process sections for base case and design alternatives (Case 1 and Case2).

Section Unit	Base Case (\$MM)	Case 1(\$MM)	Case 2 (\$MM)
HTL	28.46	45.12	45.12
SEP	14.2	12.20	12.05
STM-REF	86.28	74.60	63.68
PSA	24.20	8.11	8.11
SM-PO-CM	-	21.49	21.49
TOTAL	153.14	161.52	150.45

**Table 5.3-5.** Major material stream for Base Case and design alternatives used in the techno-economic assessment.

Material	Category	Units	Base Case	Case 2	Case 3	Ref.
Macroalgae ( <i>Saccharina Japonica</i> )	Raw Material	kg/hr		60000		[15]
Water ( Process Water )	Raw material	kg/hr		600000		[6]
Natural Gas	Utility	kg/hr	24834	9009	4000 <sup>a</sup>	[6]
HP-steam	Utility	kg/hr	124637	124637	99452	[32]
Water makeup (Steam generation)	Utility	MT/hr		216500	216500	[32]
Power	Utility	kW	3011	3685	3685	[32]
PSA Catalyst	Raw material	kg/hr	1.0252	1.0252	1.0252	[6]
Waste water treatment	Waste	gal/hr	25626	25626	25626	[32]
Solid Waste	Waste	kg/hr	7076	7076	7076	[32]
Flue gas (Carbon Tax)	Waste	kg/hr	120646	28606	28606	[34]
Power	Product	kW	0	17817	17817	[6]
LP-steam	Product	kW	0	60000	60000	[32]
Hydrogen	Product	kg/hr	6422	6520	5104	[40]

<sup>a</sup> HTL-product stream used as a combustion fuel.

**Table 5.3-6.** Manufacturing cost breakdown for Base Case, Case 1 and Case 2.

Material	Units	Base Case (\$MM)	Case 2 (\$MM)	Case 3 (\$MM)
Macroalgae (Saccharina Japonica)	kg/hr	32.64	32.64	32.64
Water ( Process Water )	kg/hr	0.34	0.34	0.34
Natural Gas	kg/hr	111.26	40.7	26.1
HP-steam	kg/hr	32.37	On-site generation	On-site generation
Water makeup (Steam generation)	MT/hr	0.00	1.73	1.73
PSA Catalyst	kg/hr	0.25	0.25	0.25
Waste water treatment	gal/hr	0.51	0.51	0.51
Solid Waste	kg/hr	20.38	20.38	20.38
Flue gas (Carbon Tax)	kg/hr	19.30	4.57	4.57
Net power	kW	0.00	9.75	9.75
LP-steam	kW	0.00	14.05	14.05
Hydrogen	kg/hr	312.96	312.96	244.99

### 5.3.5. Fixed capital investments and operating cost

The associated factors and percentages for the evaluation of the fixed capital investments are discussed in the Section 3.4. Based on those distributions the calculated costs for the design cases is shown in Table 5.3-7. Case 1 had the highest installation investment. These investments reflect additional heat exchanger for heat integrations and steam turbine. Case 1 had the highest equipment cost of 239.30 \$MM. Similarly, Case 1 had the highest value for the fixed capital investment. Despite higher investments, total operating costs for the Case 1 was lower than the Base Case design. With an increase of 10.90 % in the total installed cost for the Case 2, a decrease of 27.1 % was observed in the total operating cost. In comparison for the Case 1 with Case 2 , a further decrease of 11 \$MM in the operating cost was observed due to the modification in the fuel stream (bio-oil fraction). Variable operating costs were decreased by a huge margin of 68.1 %. The decrease in the operating cost was a result of installation of the on-site steam, heat and power generation keeping the H<sub>2</sub>-production at same level. Case 2 shows a prospective process, as the dependency on the external fuel is reduced to minimum, which is desirable for a sustainable future. The goal for the study is to evaluate lowest hydrogen selling price, design case with lowest hydrogen selling price will be considered as an optimal design for the industrial scale design.

**Table 5.3-7.** Fixed capital investment, and operating cost for design cases.

Variable	Base Case (\$MM)	Case 1 (\$MM)	Case 2 (\$MM)
Total Installation Cost (TIC)	171.21	286.81	150.48
Buildings (1% of TIC)	1.71	1.62	1.50
Site Development (9% of TIC)	15.41	14.54	13.54
Additional Piping (4.5% of TIC)	7.70	7.27	6.77
Total Direct Cost (TDC)	196.03	185.04	172.30
Prorated Expenses (10% of TDC)	19.60	18.50	17.23
Home Office and Construction Fees (20% of TDC)	39.21	37.01	34.46
Field Expenses (10% of TDC)	19.60	18.50	17.23
Project Contingency (10% of TDC)	19.60	18.50	17.23
Startup and Permits (5% of TDC)	9.80	9.25	8.61
Total Indirect Costs	107.82	101.77	94.76
Fixed Capital Investment	303.85	286.81	267.06
Land	10.27	9.70	9.03
Working Capital	15.19	14.34	13.35
Variable Operating Cost	203.16	96.37	81.73
Overhead and Maintenance (1.6% of TIC )	4.86	4.59	4.27
Maintenance Capital (3% of TIC)	3.23	3.05	2.84
Insurance and Taxes (0.7% of FCI)	21.27	20.08	18.69
Total Other Fixed Costs	31.74	30.09	28.18
Total Operating Cost	234.90	126.46	109.91

### 5.3.6. Minimum hydrogen selling price (MHSP)

Minimum hydrogen selling price for the design cases were evaluated. The minimum hydrogen selling price was calculated by making net profits zero. Profits were calculated by the difference between the manufacturing costs and the selling profit. The resultant of these two entities was considered as the net present value. The point at which there is no profit and no loss, cost of hydrogen at that point was considered as the minimum hydrogen selling price (MHSP). MHSP for the Base case, Case 1 and Case 2 is shown in Table 5.3-8.

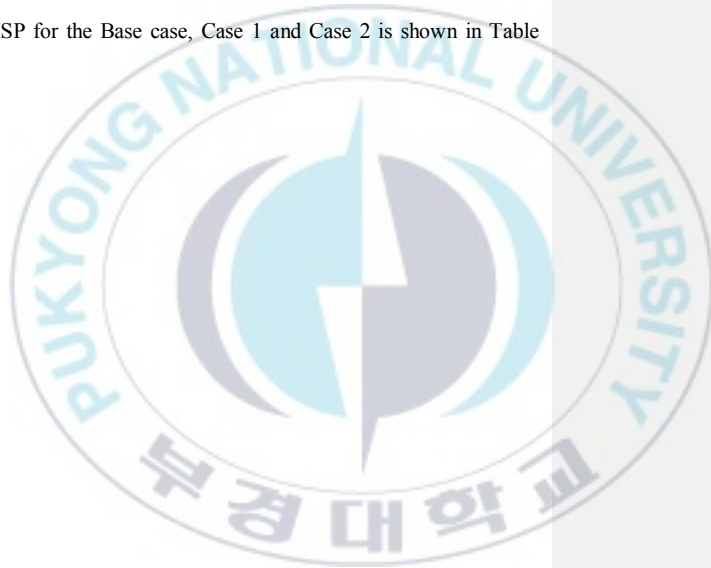
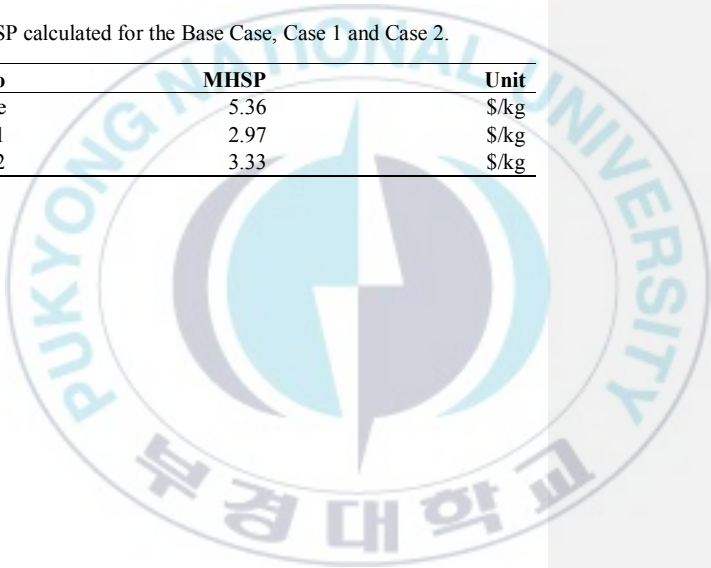


**Table 5.3-8.** MHSP calculated for the Base Case, Case 1 and Case 2.

<b>Case Scenario</b>	<b>MHSP</b>	<b>Unit</b>
Base Case	5.36	\$/kg
Case 1	2.97	\$/kg
Case 2	3.33	\$/kg



### 5.3.7. Sensitivity analysis

Impact of the economic parameters on the MHSP of the best-case scenario i.e. Case 1, is shown in Figure 5.3-3. The sensitivity analysis is based on the Case 1, with the base H<sub>2</sub> selling price of 6.0 \$/kg. Different variables were selected to see the effect on the MHSP for hydrogen. The variables chosen includes, fixed capital investment, land, working capital, income tax rate, discount rate, seaweed purchase price, natural gas and power price. Variables were varied based on their trends with the market. For variables such as seaweed, natural gas and power price these variables were varied based on the market economic assumptions. Literature support was acquired for the variation in the other economic factors i.e. FCI, discount rate etc., [6,15,34]. With 25 % decrease in the fixed capital investment, the MHSP of H<sub>2</sub> was 3.26 \$/kg, similarly with an increase of 30% in FCI, the price raised to 4.22 \$/kg. Natural gas, FCI, seaweed price, and discount rate were among the highest contributors toward the price for H<sub>2</sub>. MHSP of H<sub>2</sub> was varied between 3.48-3.93 \$/kg by varying the price of natural gas by -50% and +70% of the base price of natural gas taken in the Table 3.4-3. Highest impact was shown by the variations in the FCI, while the lowest was observed for the variations in the electricity.

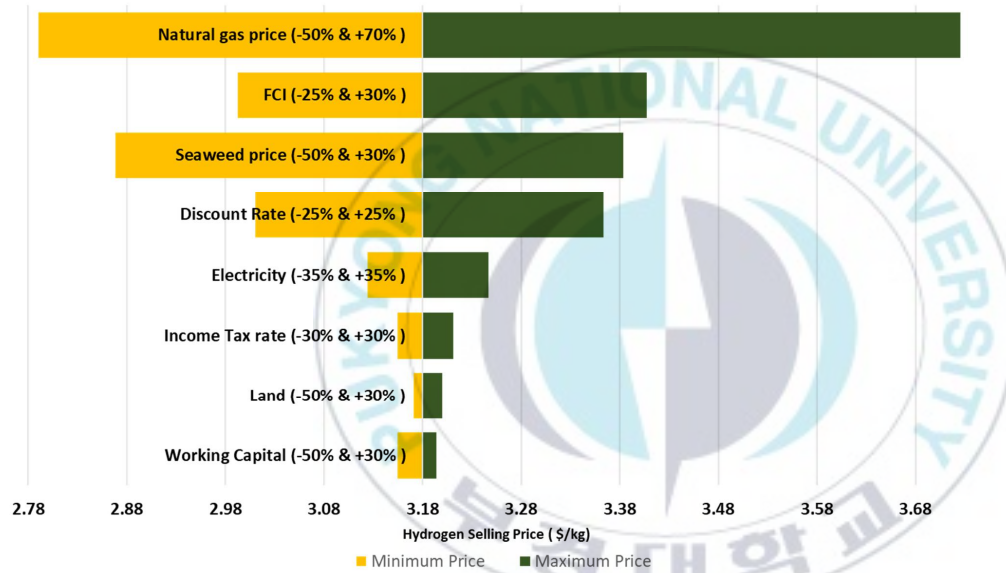


**Figure 5.3-3.** Single-point sensitivity tornado chart for minimum selling price of hydrogen by varying different variables to see the effect on the hydrogen selling price.

## CHAPTER VI

### 6 CONCLUSIONS

In this study, economic evaluation for an industrial scale H<sub>2</sub> production facility along with combined heat and power production was assessed. Feasibility study for industrial scale design of HTL using microalgae is available but for macroalgae it's still scarce. Various studies report HTL of macroalgae yielding high bio-oil yields but have lower liquefaction conversions at higher pressures of 20 MPa. More specifically for the course of our interest, studies report HTL of *Saccharina japonica* at high pressures (20 MPa) but only a few literature studies are available on HTL at autogenous pressure conditions with no economic feasibility models. Therefore, we studied the effect of various reaction parameters at lower liquefaction pressures on raw-biomass conversion and bio-oil yield. Our experimental study thus provides a support for HTL with higher conversion and relatively higher bio-oil yields in comparison to previous studies while using raw-biomass at autogenous pressure conditions. Experimental studies will lack their importance if they don't have their supporting economic studies available to evaluate these processes on industrial scale. Apparent gaps for the assessment of macroalgae as a feedstock for large scale production of biofuels via HTL are present now. Thus, to bring these technologies into reality, economic studies are required for better estimation of their viability at industrial scale. Therefore, our study tries to bridge the gaps by providing an economic

feasibility study for industrial scale process design for HTL of macroalgae based on experimental data from HTL of *Saccharina japonica* at autogenous pressure. Experimental study evaluates the highest conversion obtained for HTL based on reaction parameters. Industrial scale process design for CHHP is evaluated for downstream hydrogen production via steam reforming of the bio-oil. Process design involves heat integration with the major process sections. Keeping in mind the power requirements, on-site steam is generated from hot streams. Surplus high-pressure steam is used for power generation using steam turbine. Research innovation behind the process design for H<sub>2</sub> production via HTL of macroalgae is to make it self-sustainable by using minimum utilities and by conserving energy. A separate case scenario is evaluated in which part of bio-oil stream is utilized for replacing natural gas for combustion purposes. Cost is evaluated for various design cases to understand process economics and profits in a better way. Later, MHSP is compared for various design case scenarios for choosing the optimal design. MHSP of H<sub>2</sub> with the best-case design is reported to be 2.97 \$/kg for Case 1. Case 2 has slightly higher cost due to lesser production of H<sub>2</sub>, 3.33 \$/kg. Economic results showed that FCI, seaweed price, natural gas and discount rate had the prominent effect on the economics of the design cases. However, FCI had the highest impact. Case 1, based on the fact that, had own facility for power, steam and heat was opted as the optimal design with the MHSP.

## 다시마의 열수 액화에 기반한 삼중 발전의 기술-경제성 타당성 조사

Haider Niaz

부경대학교 일반대학원 화학공학과

### 요약

본 논문에서는 수소 생산을 위한 공급 원료 인 거대 고기 *Saccharina japonica* 의 타당성 조사가 수행되었다. 본 연구는 Aspen plus 공정 모사기를 사용하여 해조류 바이오매스의 열수액화 (hydrothermal liquefaction, HTL)를 통해 수소를 생산하는 산업 규모의 공정 설계에 대한 기술적 경제적 타당성 조사를 제공한다. 이를 위해 제품의 상 분포에 영향을 미치는 다양한 반응 매개 변수를 분석하기 위한 실험적 연구가 먼저 수행되었다. 최대 전환율은 300 °C의 반응 온도, 1 시간의 반응 시간 및 거대 조류 / 물 비율의 1:10 에서 91.2 %였다. 큰 분자의 분해를 돕는 원료의 높은 수분율 때문에 추정된다. 실험으로 얻은 제품에 대한 GC-MS 분석은 주요 작용기로서 알데히드 및 케톤을 나타냈다. 최적의 실험 조건은 공정 시뮬레이터를

사용한 공정 설계에 고려되었다. 모사 연구의 목표는 최소 수소 판매 가격 (minimum hydrogen selling price, MHSP)을 구하여 다양한 규모의 설계 사례를 평가하는 것이다. 경제성 분석을 위해 다양한 설계안들이 고려되었습니다. 다음의 여러 설계안들은 천연가스 이용을 최소화하고 열 통합을 극대화 하기위해 고안되었다: 외부의 유틸리티를 이용하는 기본 설계, 설계안 1 - 열, 수소 및 전력 병합생산 (CHHP), 사례 2 : HTL 제품의 일부를 연소용으로 사용하는 설계안 1의 변형. 설계안 1 과 2 에서 천연가스 소비를 줄이기 위해 고온 오일 시스템이 도입되었다. 열, 수소 및 전력 병합 생산 (CHHP)은 400,000 kg/yr의 젓은 *Saccharina japonica*를 원료로 사용하여 모사하였다. 설계된 공정은 HTL, 수증기 개질 (steam reforming, SRU), 압력변동흡착 (pressure swing adsorption, PSA) 및 열 및 연소 장치 등의 다양한 공정 섹션으로 구성된다. 공장은 총 유틸리티 소비를 줄이기 위해 열 통합되었다. 순 전력은 설계된 공정을 자급 자족 할 수 있도록 생산되었다. HTL로 생산된 바이오 오일의 높은 HHV(35.5 MJ/kg)로 인해 설계안 2는 연소용 연료로 바이오 오일의 일부를 사용함으로써 외부 유틸리티에 대한 의존도를 줄일 수 있었다. 프로세스의 타당성을 연구하기 위해 기술-경제성 분석이 수행되었다.

메모 포함[유1]: Correct accordingly.

경제성 분석에 따르면 설계안 1의 MHSP는 2.97 \$/kg로 가장 낮았으며 시간당 수소 생산량은 6659 kg/hr이었다. 다른 설계 사례와 비교했을 때, 설계안 1에 대한 운영 비용 및 고정 자본 투자가 적기 때문에 향후 평가에 적합하다고 판단된다.



## REFERENCES

- [1] United Nations. World Population Prospects The 2017 Revision Key Findings and Advance Tables. World Popul Prospect 2017 2017:1–46. doi:10.1017/CBO9781107415324.004.
- [2] Assadourian E, Flavin C, French H, Gardner G, Halweil B, Mastny L, et al. State of the world 2004. n.d.
- [3] OECD Environmental Outlook to 2050. OECD Publishing; 2012. doi:10.1787/9789264122246-en.
- [4] Gross M. Looking for alternative energy sources. vol. 22. 2012. doi:10.1016/j.cub.2012.02.002.
- [5] Gollakota ARK, Kishore N, Gu S. A review on hydrothermal liquefaction of biomass. Renew Sustain Energy Rev 2018;81:1378–92. doi:10.1016/J.RSER.2017.05.178.
- [6] Anderson D. Process Design and Economics for the Conversion of Algal Biomass to Hydrocarbons : Whole Algae Hydrothermal Liquefaction and Upgrading 2014.
- [7] Costanzo W, Hilten R, Jena U, Das KC, Kastner JR. Effect of low temperature hydrothermal liquefaction on catalytic hydrodenitrogenation of algae biocrude and

- model macromolecules. *Algal Res* 2016;13:53–68. doi:10.1016/j.algal.2015.11.009.
- [8] López Barreiro D, Riede S, Hornung U, Kruse A, Prins W. Hydrothermal liquefaction of microalgae: Effect on the product yields of the addition of an organic solvent to separate the aqueous phase and the biocrude oil. *Algal Res* 2015;12:206–12. doi:10.1016/j.algal.2015.08.025.
- [9] Finley M. BP statistical review of world energy. 2013.
- [10] Energy charting tool | Energy economics | BP n.d. <https://www.bp.com/en/global/corporate/energy-economics/energy-charting-tool-desktop.html> (accessed October 22, 2018).
- [11] Smil V. Energy transitions: global and national perspectives 2016.
- [12] McGill Ralph. Algae as a Feedstock for Transportation Fuels – The Future of Biofuels? Vienna: 2008.
- [13] Chen Y, Wu Y, Hua D, Li C, Harold MP, Wang J, et al. Thermochemical conversion of low-lipid microalgae for the production of liquid fuels: Challenges and opportunities. *RSC Adv* 2015;5:18673–701. doi:10.1039/c4ra13359e.
- [14] Foust TD, Aden A, Abhijit AE, Ae D, Phillips S. An economic and environmental comparison of a biochemical and a thermochemical lignocellulosic ethanol conversion processes n.d. doi:10.1007/s10570-009-9317-x.
- [15] Fasahati P, Woo HC, Liu JJ. Industrial-scale bioethanol production from brown

- algae: Effects of pretreatment processes on plant economics. *Appl Energy* 2015;139:175–87. doi:10.1016/j.apenergy.2014.11.032.
- [16] Lavanya M, Meenakshisundaram A, Renganathan S, Chinnasamy S, Lewis DM, Nallasivam J, et al. Hydrothermal liquefaction of freshwater and marine algal biomass: A novel approach to produce distillate fuel fractions through blending and co-processing of biocrude with petrocruide. *Bioresour Technol* 2016;203:228–35. doi:10.1016/j.biortech.2015.12.013.
- [17] Milledge JJ, Smith B, Dyer PW, Harvey P. Macroalgae-derived biofuel: A review of methods of energy extraction from seaweed biomass. *Energies* 2014;7:7194–222. doi:10.3390/en7117194.
- [18] Sudhakar K, Mamat R, Samykano M, Azmi WH, Ishak WFW, Yusaf T. An overview of marine macroalgae as bioresource. *Renew Sustain Energy Rev* 2018;91:165–79. doi:10.1016/j.rser.2018.03.100.
- [19] Michalak I. Experimental processing of seaweeds for biofuels. *Wiley Interdiscip Rev Energy Environ* 2018;7:1–25. doi:10.1002/wene.288.
- [20] McCook LJ. Macroalgae, nutrients and phase shifts on coral reefs: scientific issues and management consequences for the Great Barrier Reef. *Coral Reefs* 1999;18:357–67. doi:10.1007/s003380050213.
- [21] Jones SB, Holladay JE, Valkenburg C, Stevens DJ, Walton CW, Kinchin C. Production of Gasoline and Diesel from Biomass via Fast Pyrolysis, Hydrotreating and Hydrocracking: A Design Case. 2009.

- [22] Zhou D, Zhang L, Zhang S, Fu H, Chen J. Hydrothermal liquefaction of macroalgae *Enteromorpha prolifera* to bio-oil. *Energy and Fuels* 2010;24:4054–61. doi:10.1021/ef100151h.
- [23] Singh R, Bhaskar T, Balagurumurthy B. Effect of solvent on the hydrothermal liquefaction of macro algae *Ulva fasciata*. *Process Saf Environ Prot* 2015;93:154–60. doi:10.1016/J.PSEP.2014.03.002.
- [24] Chen F, Johns MR. Effect of C/N ratio and aeration on the fatty acid composition of heterotrophic *Chlorella sorokiniana*. *J Appl Phycol* 1991;3:203–9. doi:10.1007/BF00003578.
- [25] Zeb H, Park J, Riaz A, Ryu C, Kim J. High-yield bio-oil production from macroalgae (*Saccharina japonica*) in supercritical ethanol and its combustion behavior. *Chem Eng J* 2017;327:79–90. doi:10.1016/j.cej.2017.06.078.
- [26] Zeb H, Riaz A, Kim J. Understanding the effect of biomass-to-solvent ratio on macroalgae (*Saccharina japonica*) liquefaction in supercritical ethanol. *J Supercrit Fluids* 2017;120:65–74. doi:10.1016/j.supflu.2016.10.013.
- [27] Zeb H, Choi J, Kim Y, Kim J. A new role of supercritical ethanol in macroalgae liquefaction (*Saccharina japonica*): Understanding ethanol participation, yield, and energy efficiency. *Energy* 2017;118:116–26. doi:10.1016/j.energy.2016.12.016.
- [28] Anastasakis K, Ross AB. Hydrothermal liquefaction of four brown macro-algae commonly found on the UK coasts: An energetic analysis of the process and comparison with bio-chemical conversion methods. *Fuel* 2015;139:546–53.

doi:10.1016/j.fuel.2014.09.006.

- [29] Neveux N, Yuen AKL, Jazrawi C, Magnusson M, Haynes BS, Masters AF, et al. Biocrude yield and productivity from the hydrothermal liquefaction of marine and freshwater green macroalgae. *Bioresour Technol* 2014;155:334–41. doi:10.1016/j.biortech.2013.12.083.
- [30] Singh R, Balagurumurthy B, Bhaskar T. Hydrothermal liquefaction of macro algae: Effect of feedstock composition. *Fuel* 2015;146:69–74. doi:10.1016/j.fuel.2015.01.018.
- [31] Liu H-M, Li M-F. Hydrothermal Liquefaction of Cypress: Effect of Water Amount on Structural Characteristics of the Solid Residue. *Chem Eng Technol* 2014;37:95–102. doi:10.1002/ceat.201300368.
- [32] Turton, R., Bailie, R. C., Whiting, W. B., & Shaeiwitz JA. *Analysis, synthesis and design of chemical processes*. 2008.
- [33] Knorr D, Lukas J, Schoen P. Production of Advanced Biofuels via Liquefaction - Hydrothermal Liquefaction Reactor Design: April 5, 2013. Golden, CO (United States): 2013. doi:10.2172/1111191.
- [34] Dickson R, Ryu J-H, Liu JJ. Optimal plant design for integrated biorefinery producing bioethanol and protein from *Saccharina japonica*: A superstructure-based approach. *Energy* 2018;164:1257–70. doi:10.1016/j.energy.2018.09.007.
- [35] Brigljević B, Žuvela P, Liu JJ, Woo H-C, Choi JH. Development of an automated

method for modelling of bio-crudes originating from biofuel production processes based on thermochemical conversion. *Appl Energy* 2018;215:670–8. doi:10.1016/J.APENERGY.2018.02.030.

- [36] Coulson & Richardson's. *Chemical Engineering Design*. Fourth Edi. n.d.
- [37] Zhu Y, Biddy MJ, Jones SB, Elliott DC, Schmidt AJ. Techno-economic analysis of liquid fuel production from woody biomass via hydrothermal liquefaction (HTL) and upgrading. *Appl Energy* 2014;129:384–94. doi:10.1016/j.apenergy.2014.03.053.
- [38] Magdeldin M, Kohl T, Järvinen M. Techno-economic assessment of integrated hydrothermal liquefaction and combined heat and power production from lignocellulose residues. *J Sustain Dev Energy, Water Environ Syst* 2018;6:89–113. doi:10.13044/j.sdewes.d5.0177.
- [39] Wright M, Daugaard D, Satrio J, Fuel RB-, 2010 undefined. Techno-economic analysis of biomass fast pyrolysis to transportation fuels. Elsevier n.d.
- [40] Hydrogen DOE, Cell F, Bonner B. *Who is Air Products?* 2013.
- [41] Amos WA. *Biological Water-Gas Shift Conversion of Carbon Monoxide to Hydrogen Milestone Completion Report* 2004.
- [42] Park YB. *Steam Reforming of Liquefied Oil Derived from Macro Algae over Nickel-based Catalysts by Steam Reforming of Liquefied Oil Derived from Macro Algae over Nickel-based Catalysts* 니켈계 촉매를 이용한 해조류 유래

액화오일의 by. 2018.

